

WCAP-15932-NP
Revision 0

September 2002

IMPROVED JUSTIFICATION OF PARTIAL- LENGTH RPC INSPECTION OF TUBE JOINTS OF MODEL F STEAM GENERATORS OF AMEREN-UE CALLAWAY PLANT

WESTINGHOUSE NON-PROPRIETARY CLASS 3

WCAP-15932-NP

**IMPROVED JUSTIFICATION OF PARTIAL-LENGTH
RPC INSPECTION OF TUBE JOINTS OF MODEL F
STEAM GENERATORS OF AMEREN-UE CALLAWAY
PLANT**

September 2002

Westinghouse Electric Company LLC
P.O. Box 355
Pittsburgh, PA 15230-0355

© 2002 Westinghouse Electric Company LLC
All Rights Reserved

TABLE OF CONTENTS

LIST OF TABLES iii

LIST OF FIGURESv

ABSTRACT vii

1.0 INTRODUCTION 1-1

2.0 PROGRAM OBJECTIVES 2-1

 2.1 General 2-1

 2.2 Evaluation to Establish Inspection Regimen for H*/P* 2-2

3.0 ANALYSIS AND SUMMARY 3-1

 3.1 Analysis 3-1

 3.1.1 Function of H* and P* 3-1

 3.1.2 Features of H* 3-1

 3.1.3 Features of P* 3-4

 3.2 Summary 3-4

 3.2.1 H* Summary 3-4

 3.2.2 P* Summary 3-5

4.0 OPERATING CONDITIONS 4-1

 4.1 Normal Operation Conditions 4-1

 4.2 Faulted Conditions 4-1

5.0 TEST PROGRAM 5-1

 5.1 Test Sample Configuration 5-1

 5.1.1 Tubesheet Simulant (Collar) 5-1

 5.1.2 Tubing 5-2

 5.1.3 Test Sample Design Configuration 5-2

 5.1.4 Test Sample Assembly 5-2

 5.2 Test Procedure 5-3

 5.2.1 Room Temperature Primary-to-Secondary Leak Tests 5-3

 5.2.2 Elevated Temperature Primary-to-Secondary Side Leak Tests 5-3

 5.2.3 Mechanical Loading Tests 5-4

TABLE OF CONTENTS (Continued)

5.3	Test Summary.....	5-4
5.3.1	Leak Tests.....	5-4
5.3.2	Tube Pullout Tests.....	5-4
6.0	LEAK RATE EVALUATION.....	6-1
6.1	Tubesheet Constraining Effect on Crack Opening.....	6-1
6.2	Leak Rate Analysis Methodology.....	6-1
6.3	Leak Rate Results.....	6-2
7.0	STRUCTURAL ANALYSIS.....	7-1
7.1	Evaluation of Tubesheet Deflection Effects for H* and H* Leakage.....	7-1
7.1.1	Material Properties and Tubesheet Equivalent Properties.....	7-1
7.1.2	Tubesheet Rotation Effects.....	7-3
7.1.3	Callaway Contact Pressures.....	7-7
7.1.4	Summary of Results.....	7-10
7.2	Determination of Tube-to-Tubesheet Contact Pressure for H*.....	7-11
7.3	Resistance to Pullout – P*.....	7-26
7.3.1	Major Assumptions.....	7-26
7.3.2	Loads.....	7-28
7.3.3	Material Properties.....	7-28
7.3.4	Acceptance Criteria.....	7-28
7.3.5	Finite Element Models.....	7-29
7.3.6	Displacement Results.....	7-30
7.3.7	Structural Evaluation Results.....	7-32
8.0	REFERENCES.....	8-1

LIST OF TABLES

Table 3-1	Depth into Tubesheet to Meet Structural Limits for Limiting Condition (SLB)	3-6
Table 3-2	Callaway Leakage Limits (per Steam Generator)	3-7
Table 7.1-1	Summary of Material Properties Alloy 600 Tube Material.....	7-19
Table 7.1-2	Summary of Material Properties SA-508 Class 2a Tubesheet Material	7-20
Table 7.1-3	Summary of Material Properties SA-533 Grade A Class 2 Shell Material.....	7-21
Table 7.1-4	Summary of Material Properties SA-216 Grade WCC Channelhead Material	7-21
Table 7.2-1a	Maximum/Minimum Contact Pressures between the Tube and Tubesheet Including End Cap (Axial) Load on Tube at Callaway with Psec = 953 psig	7-22
Table 7.2-1b	Maximum/Minimum Contact Pressures between the Tube and Tubesheet Including End Cap (Axial) Load on Tube at Callaway with Psec = 935 psig	7-22
Table 7.2-2a	Cumulative Forces Resisting Pull Out from the Top of the Tubesheet Callaway – Hot Leg Normal Conditions – Axial Load Included, Psec = 953 psig	7-23
Table 7.2-2b	Cumulative Forces Resisting Pull Out from the Top of the Tubesheet Callaway – Hot Leg Normal Conditions – Axial Load Included, Psec = 935 psig	7-24
Table 7.2-3	Cumulative Forces Resisting Pull Out from the Top of the Tubesheet Callaway, – Faulted (SLB) Conditions – Axial Load Included	7-25
Table 7.3-1	Model F Primary to Secondary ΔP Loads Used in P* Analysis.....	7-35
Table 7.3-2	Material Properties Used in P* Analysis	7-35
Table 7.3-3	Stress Intensity Limits Used in P* Analysis.....	7-36
Table 7.3-4	Geometric Parameters Used in P* 3D FE Models	7-36
Table 7.3-5	Vertical Forces Acting on Separated Tube Leg Applied in P* FE Models	7-37
Table 7.3-6	Geometric Parameters Used in P* 1D Dynamic Fe Models	7-37
Table 7.3-7	Results of Initial Surface-to-Surface Contact Displacement Analysis.....	7-38

LIST OF TABLES (Continued)

Table 7.3-8	Total Combined Static Surface-to-Surface and Point-to-Point Contact Displacement Analysis Results for the Separated Tube Straight Leg at the Top of the Tubesheet	7-38
Table 7.3-9	Calculation of Maximum Kinetic Energy of Separated Tube at Impact with Adjacent Intact Tube for SLB Loading ($F_{SLB} = 1032$ lbf).....	7-39
Table 7.3-10	Dynamic Displacement Amplification Factors for SLB Loading ($F_{SLB} = 1032$ lbf) Calculated Using 1D Lump Mass FE Model of Figure 7.3-6	7-39
Table 7.3-11	Total Axial Primary Stress In Intact Tube Straight Legs Model F Steam Generators	7-40
Table 7.3-12	P* Primary Stress Evaluation of Intact Tube Model F Steam Generators	7-40

LIST OF FIGURES

Figure 2-1	H* Tubesheet Region Partial-RPC Justification for Steam Generators.....	2-3
Figure 2-2	P* Tubesheet Region Partial-RPC Justification for Steam Generators	2-4
Figure 3-1	H* Concept Tube Constraint in Tubesheet Only	3-8
Figure 3-2	P* Concept for SG – As Built (Tube Constraint in U-Bend).....	3-9
Figure 3-3	P* Concept Tube Constraint in U-Bend - Translated	3-10
Figure 3-4	P* Translated Tube Constraint in U-Bend at AVBs.....	3-11
Figure 3-5	Callaway Model F Tubesheet-P* Areas for Addressing Tube Separation Probability for Postulated Circumferential Cracking at Slightly More Than the RPC Depth of 3 Inches	3-12
Figure 3-6	H* Zones	3-13
Figure 5-1	Leakage Test Schematic.....	5-5
Figure 5-2	Tube Hydraulic Expansion Process Schematic.....	5-6
Figure 7-1	Finite Element Model of Model F Tubesheet Region	7-14
Figure 7.2-2a	Contact Pressures for Normal Condition at Callaway, Psec = 953 psig.....	7-15
Figure 7.2-2b	Contact Pressures for Normal Condition at Callaway, Psec = 935 psig.....	7-16
Figure 7.2-3a	Contact Pressures for FLB and SLB Conditions at Callaway, Tsec = 540.7°F	7-17
Figure 7.2-3b	Contact Pressures for FLB and SLB Conditions at Callaway, Tsec = 538.3°F	7-18
Figure 7.3-1	Schematic Showing Misalignment Between Separated and Intact Tubes at Contact.....	7-41
Figure 7.3-2	U-Bend Region Showing AVBs and Postulated Snap Through Mode Shape.....	7-42
Figure 7.3-3	Minimum Required Out-of-Plane Motion Between AVB Support Points for Postulated Snap Through.....	7-43

LIST OF FIGURES (Continued)

Figure 7.3-4A	In-Plane View FE Deformed Geometry Plot of Postulated Snap Through at Nodes 68, 77 and 85 Used to Obtain Minimum Strain Energy Required to Establish Snap Through.....	7-44
Figure 7.3-4B	Out-of-Plane View FE Deformed Geometry Plot of Postulated Partial Snap Through at Nodes 68, 77 and 85 Used to Obtain Minimum Strain Energy Required to Establish Snap Through.....	7-45
Figure 7.3-5A	FE Model – [] ^{a,c,e} 7-46
Figure 7.3-5B	FE Model – [] ^{a,c,e} 7-47
Figure 7.3-5C	FE Model – [] ^{a,c,e} 7-48
Figure 7.3-6	[] ^{a,c,e} 7-49
Figure 7.3-7	Geometry of Initial (1st) Surface-to-Surface Contact Between Separated and Intact Tubes.....	7-50
Figure 7.3-8	Static Point-to-Point In-Plane Displacement Vectors of Rows 4/5 U-bend Region Separated and Intact Tubes for [] ^{a,c,e} 7-51
Figure 7 3-9	Static Point-to-Point In-Plane Displacement Vectors of Rows 30/31 U-bend Region Separated and Intact Tubes For [] ^{a,c,e} 7-52
Figure 7.3-10	Static Point-to-Point In-Plane Displacement Vectors of Rows 58/59 U-bend Region Separated and Intact Tubes For [] ^{a,c,e} 7-53
Figure 7 3-11	Time History Displacement Response of Rows 4/5 Separated and Intact Tubes for [] ^{a,c,e} 7-54
Figure 7.3-12	Time History Displacement Response of Rows 30/31 Separated and Intact Tubes For [] ^{a,c,e} 7-55
Figure 7.3-13	Time History Displacement Response of Rows 58/59 Separated and Intact Tubes For [] ^{a,c,e} 7-56

ABSTRACT

Justifications were developed to reduce the RPC inspection length of Model F steam generator tubes within the tubesheet from full-length to partial-length for the Callaway Plant. The criteria are referred to as partial-length RPC justifications.

The H* justification shows that, based on plant observance of a certain maximum primary-to-secondary side leakage value during normal operation, PWSCC below a certain depth into the tubesheet from the tubesheet top will pose neither structural issues such as tube separation and pull-out nor excessive leakage during the limiting accident condition, steamline break. If or when the normal operation leakage reached the certain maximum level, the plant would plug the leaking tubes, preferably during a refueling outage. An evaluation has been performed to develop the certain RPC inspection depth, known as H*, below which any type of axial or circumferential PWSCC can be accommodated providing normal operation leakage is closely monitored. The determination of H* consists of analyses and testing programs which quantified the tube-to-tubesheet hole surface radial contact pressure of the Westinghouse Model F steam generator tubes for the bounding plant conditions. The tube within the H* length must be undegraded and is verified as such in the periodic RPC inspection programs. H* is reckoned downward from the top of the tubesheet and assumes a conservative distance between the bottom of the hydraulic expansion transition and the top of the tubesheet. (A case-by-case accommodation of tube joints is recommended if manufacturing variabilities result in the transition bottom being located slightly below the conservative extent below the tubesheet top surface.)

H* varies with distance of a particular tube from the vertical centerline of the tube bundle. The tubes are grouped in four zones, based on distance from the bundle vertical centerline. H* varies from 2.38 to 7.98 inches. Due to tubesheet upward bending during normal operation and during the limiting accident condition, the tube-to-tubesheet hole surface contact pressure varies through the thickness of the tubesheet. The resistance to leakage through a crack and through the tube-to-tubesheet interface to the secondary side is a function of fluid conditions and tube-to-tubesheet contact pressure. Therefore, leakage from a given crack in a given tube is a function of a crack distance from the tubesheet top and tube distance from the bundle (tubesheet) vertical centerline.

An additional portion of the justification for partial-length RPC inspection of the tube joint is P*. P* was determined to be 3 inches, reckoned downward from the tubesheet top. The main function of P* is to act as a contingency for potential circumferential cracks slightly below the existing 3 inch RPC inspection depth. The intent of P* is to show the acceptability of a tube separation below the P* distance for approximately 95 percent of the operating tubes in the bundle. P* is based on the consideration that an affected tube will be captured by the non-degraded neighboring, next-larger-radius-row tube in the same column, thus limiting the vertical motion that could ensue if the tube separated within the tubesheet and maintaining a small engagement with the tubesheet hole. The engagement ranges from 0.30 inch to 1.4 inches and depends on the distance of a tube from the tube bundle vertical centerline.

NOMENCLATURE

AFT	Away-From (Hydraulic Expansion) -Transition
ASME	American Society of Mechanical Engineers
BC	Bobbin Coil
BET	Bottom of (Hydraulic) Expansion Transition
CL	Cold Leg
CP	Contact Pressure
ECT	Eddy Current Test
FLB	Feed Line Break
FSAR	Final Safety Analysis Report
gpd	Gallons per Day
gpm	Gallons per minute
H*	H-Star
HET	Hydraulic Expansion Transition
HL	Hot Leg
ID	Inside Diameter
Callaway	AmerenUE Callaway Plant
N/A	Not Applicable
NDE	Non-Destructive Examination
NOP	Normal Operation
OD	Outside Diameter
P*	P-Star
PRJ	Partial-Length RPC Justification
PLRPC	Partial-Length RPC
PWSCC	Primary Water Stress Corrosion Cracking
Q	Water Flow
R_o	Outboard Radius of a Zone Boundary
RCS	Reactor Coolant System
RPC	Rotating Pancake Coil

NOMENCLATURE (Continued)

SLB	Steamline Break
TS	Tubesheet
TT	Thermally Treated
TTS	Top of Tubesheet
V	Volts
γ_s	Inspection Depth Based on Structural Requirements (structural pull-out resistance)
γ_{ZCP}	Axial Extent of Joint with Zero Contact Pressure Between Tube and TS Hole Surface
$\gamma_{N, SLB}$	Inspection Depth for a given zone (N), SLB

1.0 INTRODUCTION

NRC Information Notice 98-27 pointed out that steam generator (SG) repair criteria often require licensees to consider the entire length of the tube in determining whether or not tubes are degraded or defective. The widely used bobbin coil nondestructive examination (NDE) process appears to be inadequate for the detection and/or sizing of many types of degradation in the "full-depth" region of the tube-to-tubesheet joint and in the tube end region. This means that, tube corrosion (cracking, particularly circumferential), if present, could be inadequately detected or its size measured by the bobbin coil (BC) probe. However, the performance of an extensive rotating pancake coil (RPC) inspection of the tube within the tubesheet can be demonstrated to be technically unnecessary for the most part. Moreover, it has been observed that performing RPC inspection over a significant extent of the full-depth of the tube joint requires excessive time during the plant outage. Developing and implementing an improved, rapid, reliable, non-RPC process is not practical with current inspection technology. Therefore, in lieu of using rotating pancake coil (RPC)¹ probes in the vicinity of the tube weld and/or to inspect for degradation at all elevations within the full-depth below the top of the tubesheet, it is recommended that partial-length RPC (PLRPC) inspection be performed only for a distance of 3 inches reckoned down from the top of the tubesheet. Due to primary water stress corrosion cracking (PWSCC) already having been documented in the region between the hydraulic expansion transition bottom and the 3 inch depth in the Callaway SGs, it is recommended to use the PLRPC justification developed herein and to inspect to the associated non-full-depth lengths determined in this evaluation.

The purpose of this report is to document the development of a technical justification for the application of PLRPC inspection of the tube within the tubesheet. There are two components, designated H* and P* (referred to as H-star and P-star respectively), of the technical rationale for application of PLRPC to address potential cracking below the elevation of the RPC zone for the Callaway Model F SGs.

H* is the sound length of tube-to-tubesheet joint required to prevent pullout of the tube from the tubesheet and to limit primary-to-secondary leakage to acceptable levels at the limiting SG condition, i.e., the steamline break condition. The implementation of H* involves performing PLRPC of the tube within the tubesheet to average depths comparable to the currently specified depth of 3 inches (on average for all of the tubes on the hot leg). The application of H* is invoked if PWSCC is suspected, or confirmed, to be occurring within the tubesheet or when it is concluded there is a not insignificant potential for such occurrence. In the case of Callaway, PWSCC within the trigger region of the tube, i.e., below the bottom of the hydraulic expansion transition and the standard 3 inch inspection depth, has been determined by NDE.

The mechanical features of the existing tube-to-tubesheet joint have been analyzed and have been shown able to perform the mechanical and hydraulic functions of the tube joint including and below the elevation of H*, including the function of the weld. The H* joint would provide adequate resistance to

¹ The RPC probe referred to herein is the Zetec™ +Point (plus point) probe.

[

] ^{a,c,e}

In the case of leakage resistance, cracks at various depths below H* are hypothesized and conservative leakage for types and numbers of cracks is projected and compared with the practical normal operation primary-to-secondary side limit and with the corresponding, bounding, accident leakage limit, SLB. A similar approach has been demonstrated to be acceptable for use in cases of tube weld damage due to loose parts. In those cases, the entire length of the hydraulically expanded tube joint, above the weld, was demonstrated to be adequate to replace the potentially ineffective weld. For reasons to be discussed later, the numerical value of H* is a function of radius from the vertical centerline of the tubesheet.

P* is based on the consideration that an affected tube will be captured by the [

] ^{a,c,e}. The P* length is less than the H* length in some regions of the tube bundle.

The improved justification approach to address tube PWSCC in the tube joint, the limiting or most severe case of which is [

] ^{a,c,e}. In the past, the RPC area typically extended downward approximately 3 inches from the top of the tubesheet. (It depends on customer definition in the outage ECT contract.) In this case, the lower, approximately 18 inches of the tube in the tubesheet is in what is referred to as the bobbin coil (BC) zone or reduced-inspection-accuracy zone.

The intent of the P* portion of the justification is to show the acceptability, on the basis of [

] ^{a,c,e}. P* and H* were developed as a contingency because tube PWSCC may be anticipated due to the relatively high T-hot of the Model F SGs, which may cause the tubing to be subject to potential degradation in the BC zone. Some of the logic and data used to develop H* were also used to clarify the features of P*.

2.0 PROGRAM OBJECTIVES

2.1 GENERAL

The purpose of this program is to define a tube inspection length in the SG tubesheet below which no special nondestructive examination of the SG tubes needs to be performed and, ultimately, to provide the basis for a Technical Specifications change to that effect should one be required. It is to be based on the development of partial-length RPC justification criteria referred to as H* and P*.

Based on the results of this evaluation, and the results of several inspections during refueling outages wherein PWSCC (axial and circumferential) was indicated in the region between the hydraulic expansion transition bottom and the 3 inch RPC inspection depth, it is recommended that the RPC inspection length of the tube within the tubesheet be the H* lengths. (Note: The region between the transition bottom and the 3 inch depth is referred to as the away-from-transition, or AFT, region.) In the case of one zone where H* is less than 3 inches, consideration may be given to keeping the RPC depth at the existing three inch length reckoned down from the top of the tubesheet (TTS).

It is assumed that the transition axial extent is taken as approximately [

] ^{a,c,e}

below the TTS, consideration may be given to adjusting the RPC inspection depth for that tube.)

It is recommended that the initiation of inspection to H* depths also initiate the use of P*.

Because primary side tube cracking has already been found in the AFT region of the Callaway SGs, the inspection minimum axial extent should be the H* values (per Table 3-1) for the tubes to be inspected.

The [

] ^{a,c,e}. The H* PLRPC is shown on Figures 2-1, 3-1 and 3-6
and P* is shown on Figures 2-2, 3-2 through 3-5.

P* provides a contingency against [

] ^{a,c,e} with the tubesheet hole for all SG conditions.

2.2 EVALUATION TO ESTABLISH INSPECTION REGIMEN FOR H*/P*

Assumptions used for establishing H* and P*:

- Bobbin coil ECT is capable of detecting a separated tube, i.e., circumferential cracking and deep axial indications (+Point with a peak-to-peak voltage amplitude, V_{pp} , >3 V) within the tubesheet.
- Some potential normal operation (NOP) leakage from a separated tube is acceptable because such a severe crack would not be expected to appear suddenly, and, hence, the leak rate would start small, would be detectable, and would only gradually reach the maximum practical NOP leakage of 75 gpd.
- Tube cracking within the tubesheet is PWSCC.
- The separated tube condition for H* and P* is a low probability event for hydraulic expanded Alloy 600 mill annealed and thermally treated tubing.
- H* distances will prevent [
$$]^{a.c.e}$$
- P* distances will prevent the probability of [
$$]^{a.c.e}$$
 RPC inspection depth.
- Crack growth is manageable over the inspection interval (two cycles – based on examining the tubes in two of the four SGs each refueling or inspection outage and a 50% RPC program in the HL of each of the opened SGs).
- The maximum allowable primary-to-secondary side leakage during the limiting accident condition, i.e., Steamline Break (SLB), through the affected SG is 1.0 gpm in the affected SG.
- The plant primary side makeup capacity is on the order of 100 gpm.



Figure 2-1
H* Tubesheet Region Partial-RPC Justification For Steam Generators

a.c.e

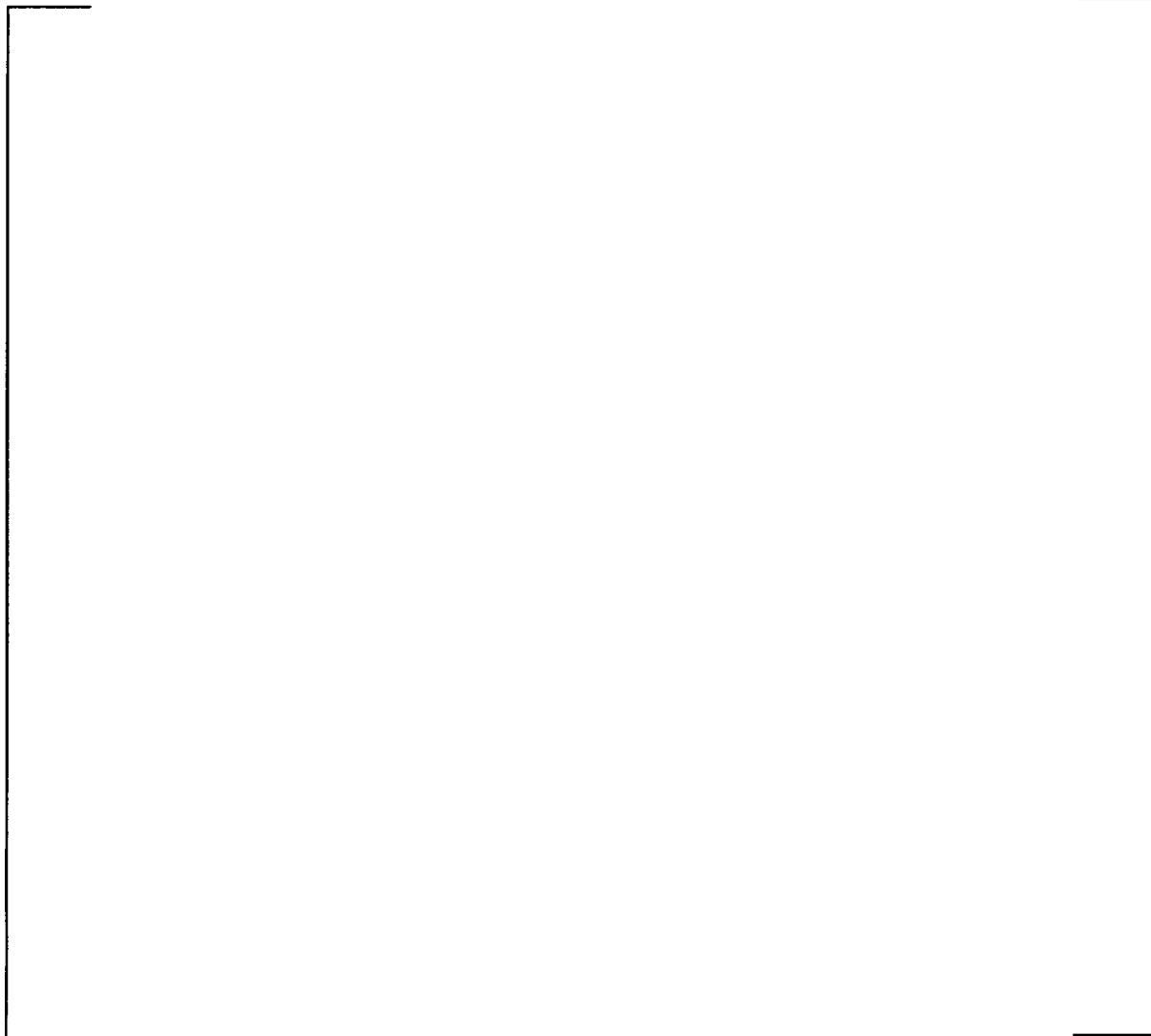


Figure 2-2
P* Tubesheet Region Partial-RPC Justification for Steam Generators

3.0 ANALYSIS AND SUMMARY

3.1 ANALYSIS

3.1.1 Function of H* and P*

Because PWSCC has been indicated within the three-inch RPC inspection depth of the Callaway SGs, it is recommended to implement inspection to the H* depths. More specifically, circumferential and axial cracking has been indicated in the "trigger" region between the tube hydraulic expansion transition bottom and the three-inch inspection depth, i.e., the "away-from-transition" (AFT) region. (Note: The H* depths are less than 3.00 inches in one of the four zones and greater than 3.00 inches in the other three zones. Refer to Figures 2-1 and 3-1 and Table 3-1 determined in this evaluation.)

The P* justification addresses the very small likelihood of [

] ^{a,c,e}, where P* is permitted are shown on Fig. 3-5.

3.1.2 Features of H*

3.1.2.1 Leakage Resistance

The HL-only RPC inspection program for the tubes in the opened SGs is assumed. The following logic has been developed for addressing potential leakage:

Single Axial Crack:

For a single axial crack in a given zone of the tubesheet such as Zone B (approximately 30.2 inches from the TS vertical centerline) and for the local H* based on [

.] ^{a,c,e}

Multiple Axial Cracks:

The same, bellweather, logic which holds for a single axial crack will also hold for multiple axial cracks. In this case, for [

] ^{a,c,e}, to accumulate to the 1.0 gpm accident leakage limit. The margin would be greater in Zone A.

Circumferential Cracks:

Circumferential cracks will also conform to [

] ^{a,c,e}.

Past experience with circumferential cracks inside the TS, for another type of tube joint, i.e., not hydraulic expansion joints, infers that leakage is low. The same trend is expected for the Callaway hydraulic expanded joints.

3.1.2.2 Tube Anchorage

Given that PWSCC has been indicated in the AFT region of the Callaway SGs, H* is recommended to be used for all of the tubes during the upcoming outage and in future outages. While it is impossible to prevent an increase over the past three-inch inspection depth over roughly 70 percent of the tubesheet, based upon the available data, the scope and impact of that expanded inspection length can be minimized. It is, therefore, recommended that the tubesheet be divided into [

] ^{a,c,e}

An example of the calculation of H*, based on structural requirements, for the zone (designated Zone D) closest to the TS vertical centerline will be presented:

Accident (SLB) condition:

The inspection distance consists of the tube-to-tubesheet contact pressure area and the zero contact pressure area:

(From Section 7)

[^{a,c,e}

[^{a,c,e}

[^{a,c,e}

[^{a,c,e}

The [

] ^{a,c,e}, for simplicity in

implementation.

The same type of calculation is made and discussed for NOP to show the logic which was used:

Normal Operation Condition:

The depth for the structural criterion for normal operation, [

] ^{a,c,e}.

Determination of H* for a Zone

H* for each zone is determined as the inspection depth based on [] ^{a,c,e}.

The inspection depth-versus-R relationship is [

] ^{a,c,e}. The H* information is summarized in Tables 3.1 and 3.2.

The bobbin probe would be used to look for a separated tube condition or large axial indications, +Point $V_{pp} > 3$ V, would be used within the tubesheet and below the RPC inspection depth. The signals identified by bobbin would be further interrogated by RPC in order to characterize them and to separate them from potential false positives (e.g. expansion anomalies).

The RPC inspection depths and the locations of any detected crack-like indications would need to be reviewed to determine whether they should be extended to provide an additional buffer zone. It is assumed that all of the tubes in the 50 percent program of the opened SGs would be inspected to the H* depth.

3.1.3 Features of P*

[

are shown in Section 7.3.]^{a.c.e.} The details of the P* analysis

The application of the P* criterion to any one tube requires that the [

]^{a.c.e.}

3.2 SUMMARY

3.2.1 H* Summary

In this configuration, the following is assumed :

1. Consider multiple tubes in a given SG to be degraded (The incidence of ID cracking in the A600TT tube hydraulic expansion joints in Callaway SGs is very low and for the tubes in other plants of any diameter, such as 11/16 inch, 3/4 inch or 7/8 inch appears to be very low.)
2. For normal operation, the plant will operate as long as the leak rate stays []^{a.c.e.}
3. For the accident condition (steamline break/feedline break – SLB/FLB):

$Q_{SLB/FLB} = 1.0$ gpm for the affected SG

Note: []^{a.c.e.}

4. It is considered to be impossible to [

] ^{a,c,e}.

Justifications were developed to reduce the RPC inspection length of the Model F steam generator tubes within the tubesheet from full-length to partial-length for the Callaway Plant. The criteria are referred to as partial-length RPC justifications and show that, based on plant observance of a [

] ^{a,c,e}.

An evaluation has been performed to develop the certain RPC inspection depth, known as H*, [

] ^{a,c,e}. The H* values do not contain any margin for NDE uncertainty in elevation of the crack features.

The tubes are grouped in [

] ^{a,c,e}.

3.2.2 P* Summary

P* approximates 3 inches, [

] ^{a,c,e}.

[

] a.c.e.

P* Evaluation Features - Summary

Addresses case of [

•

] a.c.e.

Table 3-1
Depth into Tubesheet to Meet Structural Limits for Limiting Condition (SLB)

a.c.e

Table 3-2

Callaway Leakage Limits (Per Steam Generator)

Operating Condition	Leakage Limits Maximum Per SG		
	Tech. Spec.	FSAR	Administrative
Normal Operation	500 gpd (0.35 gpm)	N/A	150 gpd (0.104 gpm)
SLB/FLB	N/A	¹ 1440 gpd (1.00 gpm)	N/A
Notes:			
1) The 1.0 gpm FSAR leakage applies only to the faulted loop.			
2) Negligible secondary-to-primary side leakage is acceptable during LOCA.			

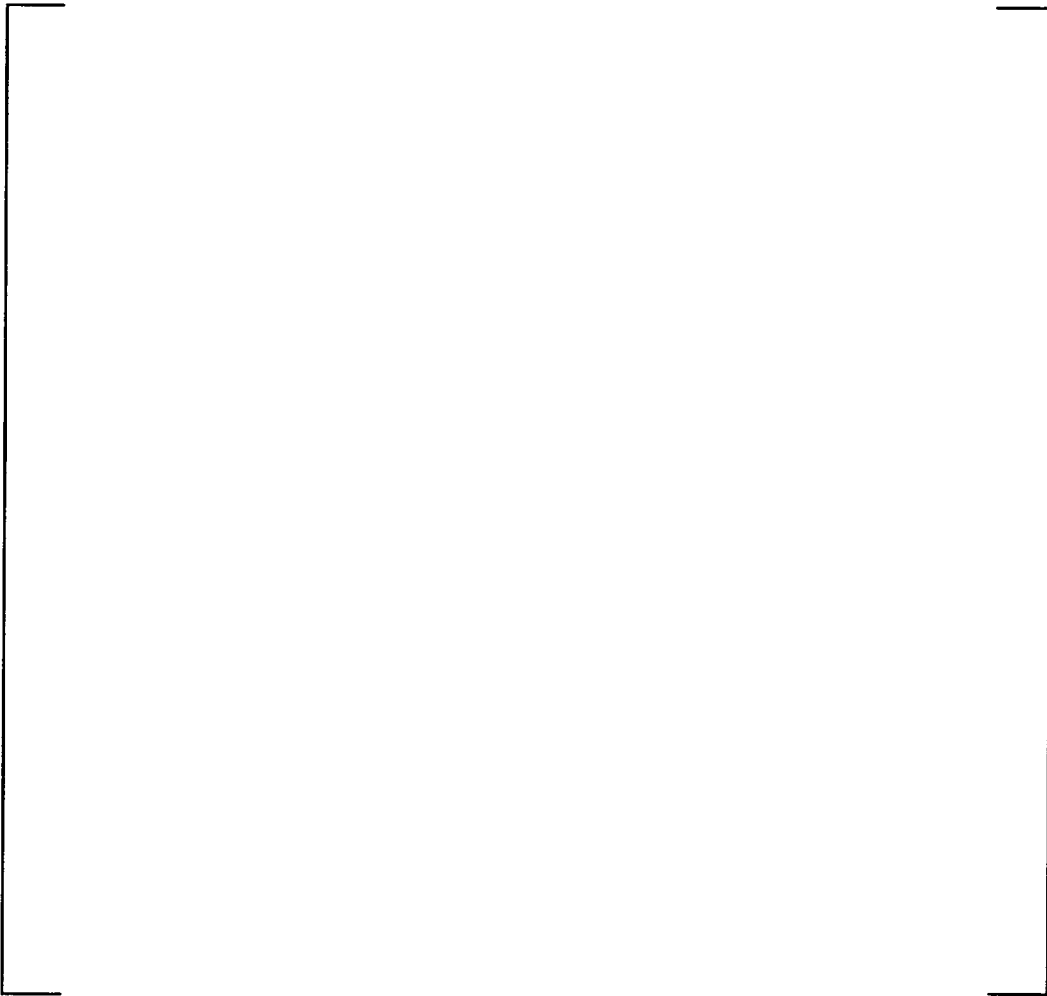


Figure 3-1
H* Concept Tube Constraint in Tubesheet Only

a.c.c

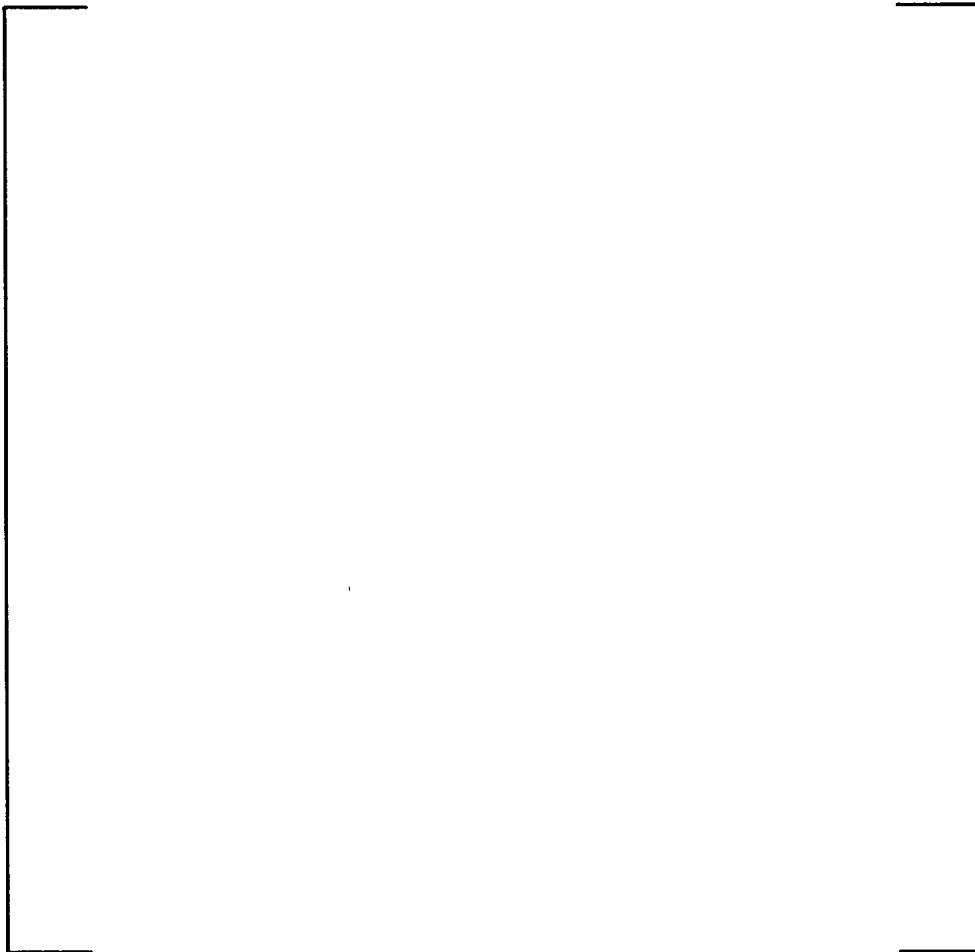


Figure 3-2
P* Concept for SG -- As Built (Tube Constraint in U-Bend)

a.c.e



Figure 3-3
P* Concept Tube Constraint in U-Bend - Translated



Figure 3-4
P* Translated Tube Constraint in U-Bend at AVBs

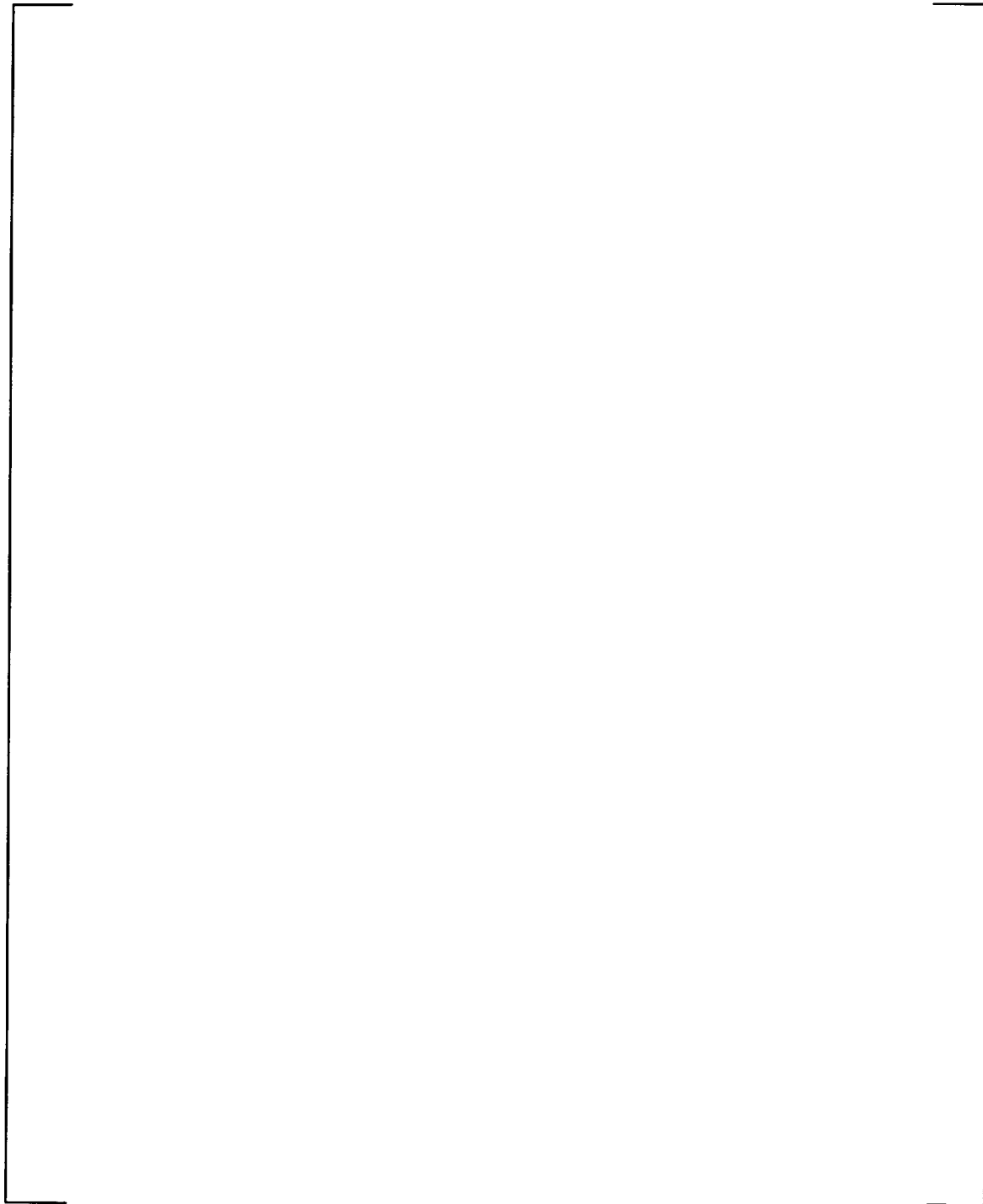
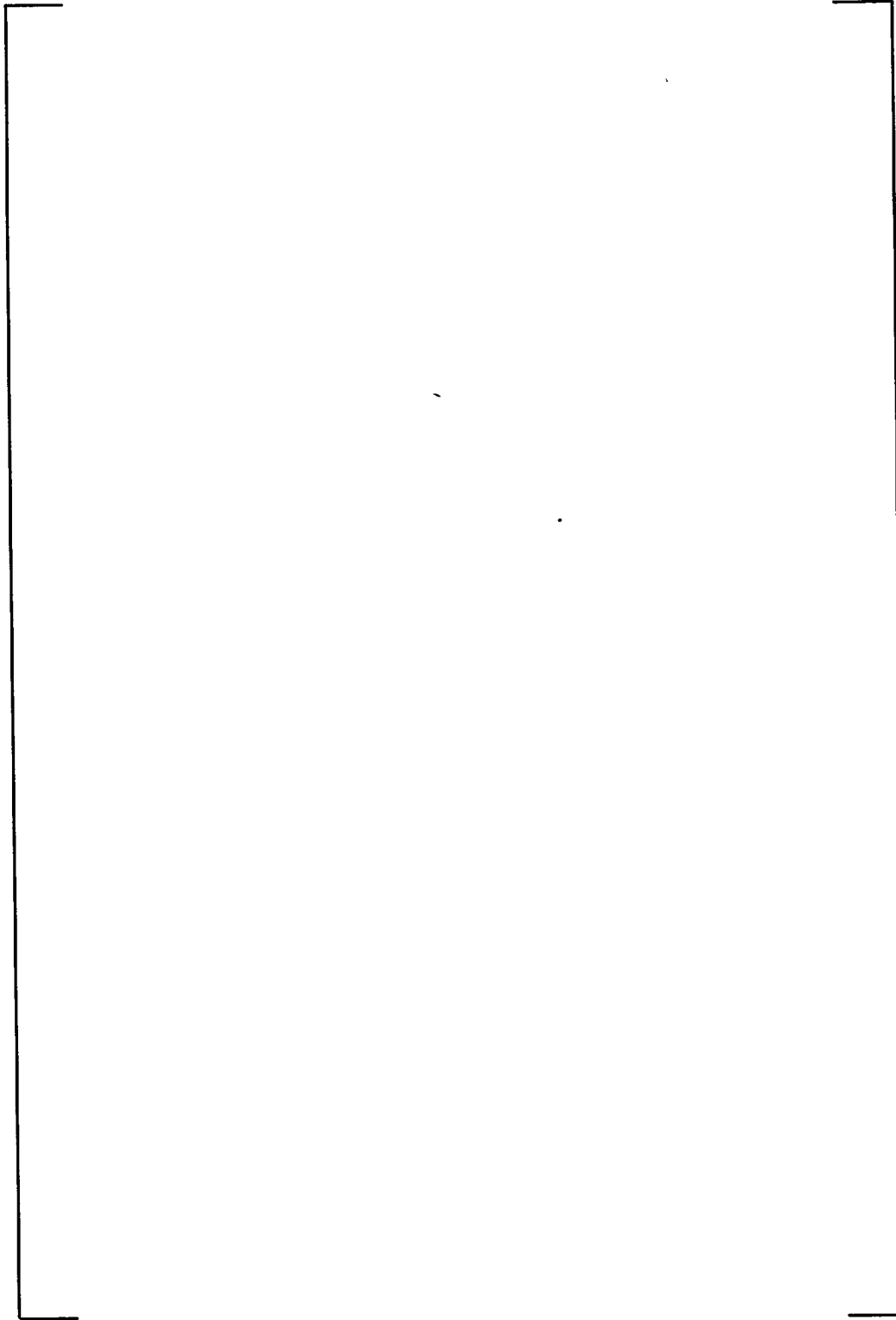


Figure 3-5
Model F Tubesheet -P* Areas for Addressing Tube Separation Probability for Postulated Circumferential Cracking at Slightly More Than the RPC Depth of 3 In.

a,c,e



H* Zones: [

Figure 3-6

]a,c,e

4.0 OPERATING CONDITIONS

Callaway Unit 1 is a four-loop plant with Model F steam generators.

4.1 NORMAL OPERATION CONDITIONS

Values of the plant thermal and hydraulic parameters during normal operation at 10 percent tube plugging conditions applicable to this study are tabulated below:

Parameter	Units	Normal Operation Conditions ⁽¹⁾	
		Case 2 ⁽²⁾	Case 3 ⁽³⁾
Power – NSSS	MWt	3579	3579
Reactor Vessel Outlet Temperature	°F	615.3	620.0
Reactor Coolant System Pressure	psia	2250	2250
SG Steam Temperature	°F	533.0	540.8
SG Steam Pressure	psia	908	970

(1) Reference 8.10

(2) Minimum Steam Temperature and Pressure in Reference 8.10

(3) Maximum Steam Temperature and Pressure in Reference 8.10

4.2 FAULTED CONDITIONS

In addition to the RG 1.121 criteria, it is necessary to satisfy FSAR accident condition values for primary-to-secondary leak rates. Calculated primary-to-secondary side leak rate during postulated events should: 1) not exceed the total charging pump capacity of the primary coolant system, and 2) be such that the off-site radiological dose consequences do not exceed title 10 of the code of federal regulations (10 CFR) Part 100 guidelines.

The accident condition primary-to-secondary leakage must be limited to acceptable values established by plant specific final safety analysis report (FSAR) evaluations. The appropriate value for the Callaway SGs is 1.0 gpm for the affected SG. Pressure differentials associated with a postulated accident condition event can result in leakage from a throughwall crack through the interface between a hydraulically expanded tube in the tubesheet and the tube hole surface. Therefore, a steam generator leakage evaluation for faulted conditions is provided in this report. The accidents that are affected by primary-to-secondary leakage are those that include, in the activity release and off-site dose calculation, modeling of leakage and secondary steam release to the environment. Steamline break (SLB) is the limiting condition; the reasons that the SLB is limiting are: 1) the SLB primary-to-secondary leak rate in the faulted loop is assumed to be greater than the operating leak rate because of the sustained increase in

differential pressure, and 2) leakage in the faulted steam generator is assumed to be released directly to the environment. For evaluating the radiological consequences due to a postulated SLB, the activity released from the affected SG (which is connected to the broken steam line) is released directly to the environment. The unaffected steam generators are assumed to continually discharge steam and entrained activity via the safety and relief valves up to the time when initiation of the RHR system can be accomplished. A 1.0 gpm (1440 gpd) primary-to-secondary leakage is assumed for the affected SG, which is significantly greater than that anticipated during normal operation. Furthermore, the radiological consequences evaluated, based on meteorological conditions, assumed that all of this flow goes to the affected steam generator. With this level of leakage, the resultant doses are well within the guideline values of 10 CFR 100.

5.0 TEST PROGRAM

The test program, see Reference 8.1, had two purposes:

1. To determine the [

]a.c.e.

5.1 TEST SAMPLE CONFIGURATION

The intent of the test samples was to model key features of the Model F tube-to-tubesheet joint for []a.c.e. The following hardware was used:

5.1.1 Tubesheet Simulant (Collar)

The collar simulates the circumferential stiffness of a Model F tubesheet unit cell, utilizing an appropriate outside diameter of approximately [

]a.c.e.

5.1.2 Tubing

The yield strength for the SG Alloy 600 tubing ranges between []^{a,c,e}. The Alloy 600 tubing used for these tests was from a certified heat and lot conforming to ASME SB163, Section III Class 1. It was obtained from a Quality Systems-controlled Storeroom. This material had a yield strength of []^{a,c,e} ksi, making yield strength-sensitive test results appropriate.

5.1.3 Test Sample Design Configuration

The intent of the leakage portion of the test program was to determine the leakage resistance of simulated Model F tube-to-tubesheet joints, disregarding the effect of the tube-to-tubesheet weld and the []

[]^{a,c,e}. (These welds were an artifact of the test design and did not affect the test condition because they made no contribution to hydraulic resistance from the tube-to-tubesheet weld or the tube tacking operation.)

5.1.4 Test Sample Assembly

5.1.4.1 Tube Tack Rolling Operation

The steam generator factory tubing drawing specifies a []

[]^{a,c,e}, to facilitate the weld to the cladding on the tubesheet face.

The assembly of the test samples required an appropriate roll expansion torque to bring the tube into light contact with the collar. Wall thinning calculations performed on the tacked region of the tube show values of no more than []^{a,c,e}. This indicates a lack of significant contact with the collar, and conformance with the intent of the factory tacking operation

5.1.4.2 Tube Hydraulic Expansion

The hydraulic expansion pressure range for the Callaway steam generators was approximately []

[]^{a,c,e}

[]^{a,c,e}. This value conservatively bounds the lower expansion pressure limit used for the Callaway steam generators.

The tube expansion tool used in the factory consisted of a pair of seals, spaced by a tie rod between them. The hydraulically expanded zone was positioned relative to the lower surface of the tubesheet, overlapping the upper end of the tack expanded region. It extended to within a short distance of the upper surface of the tubesheet. This produced a hydraulically expanded length of approximately []^{a,c,e} inch nominal tubesheet depth.

The majority of the test samples were fabricated using []

[]^{a,c,e}. These samples are described as "Segmented Expansion" types. A tube expansion schematic is shown in Figure 5-2.

A small group of the test samples were fabricated using a []^{a,c,e} tool which was fabricated expressly for these tests. These samples were described as "Full Depth Expansion" types. The expansion method with regard to the segmented or full length aspect does not have a bearing on the test results.

5.2 TEST PROCEDURE

The testing reported herein was performed according to a test procedure which outlined two types of leak tests and one mechanical loading test. The tests performed are described below.

5.2.1 Room Temperature Primary-to-Secondary Leak Tests

Room temperature primary-to-secondary leak tests were performed on all test samples, using deionized water as a pressurizing medium. []

[]^{a,c,e}, to simulate the lack of a tube weld.

5.2.2 Elevated Temperature Primary-to-Secondary Side Leak Tests

Elevated temperature primary-to-secondary side leak tests were performed using an []^{a,c,e}

[

] ^{a.c.e.}

These tests were performed following the room temperature primary-to-secondary side leak tests on the chosen samples. The test results showed a [

] ^{a.c.e.}

5.2.3 Mechanical Loading Tests

Mechanical loading, [

] ^{a.c.e.}

5.3 TEST SUMMARY

5.3.1 Leak Tests

The room temperature leak tests on nominal diameter segmented expansion collars averaged [

] ^{a.c.e.} (As a point of reference, there are approximately 75,000 drops in one gallon.) The general use of these results in the projection of leakage from postulated cracks during operation of Callaway is discussed in Section 6.0.

5.3.2 Tube Pullout Tests

[

] ^{a.c.e.}

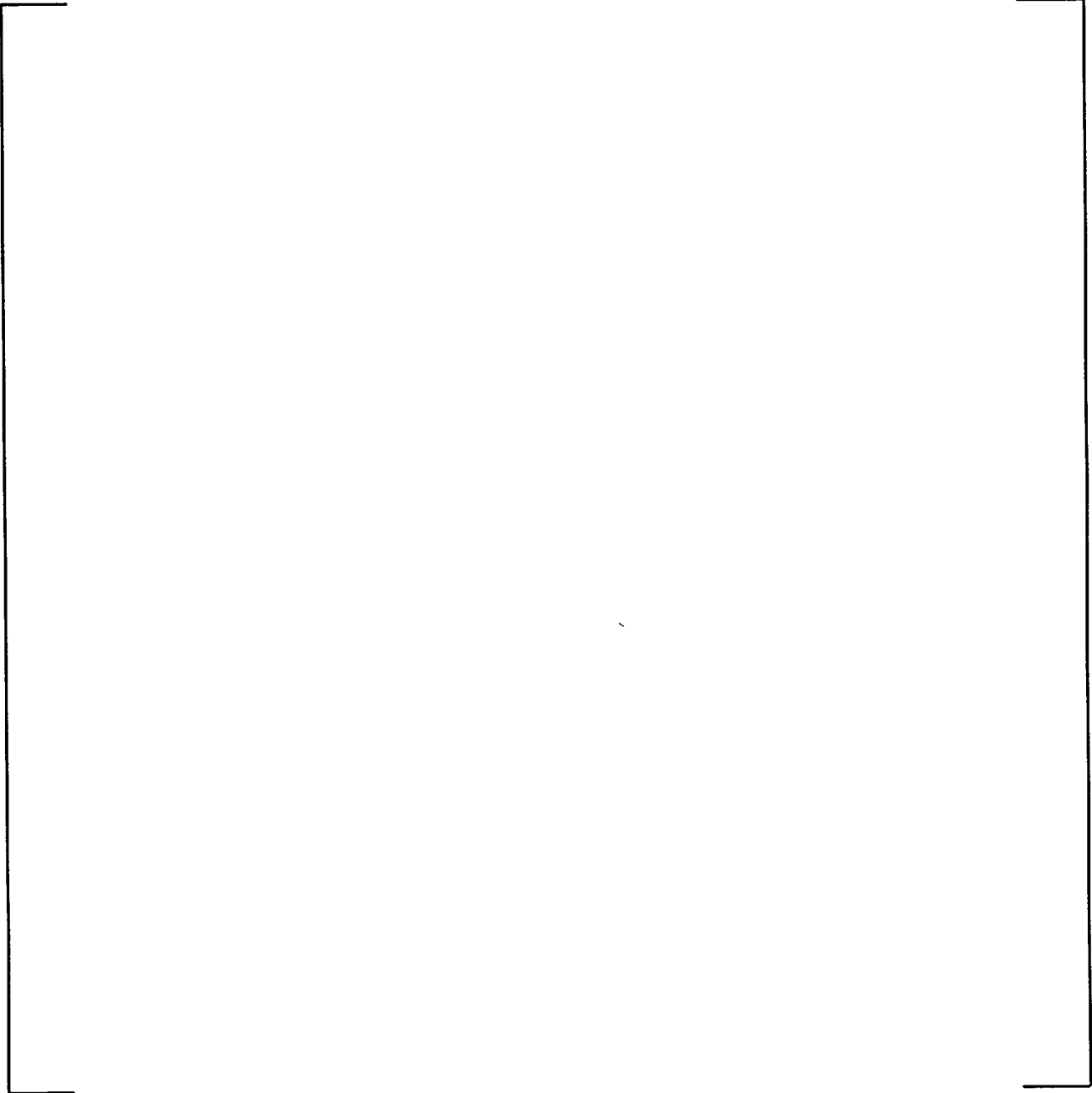


Figure 5-1
Leakage Test Schematic

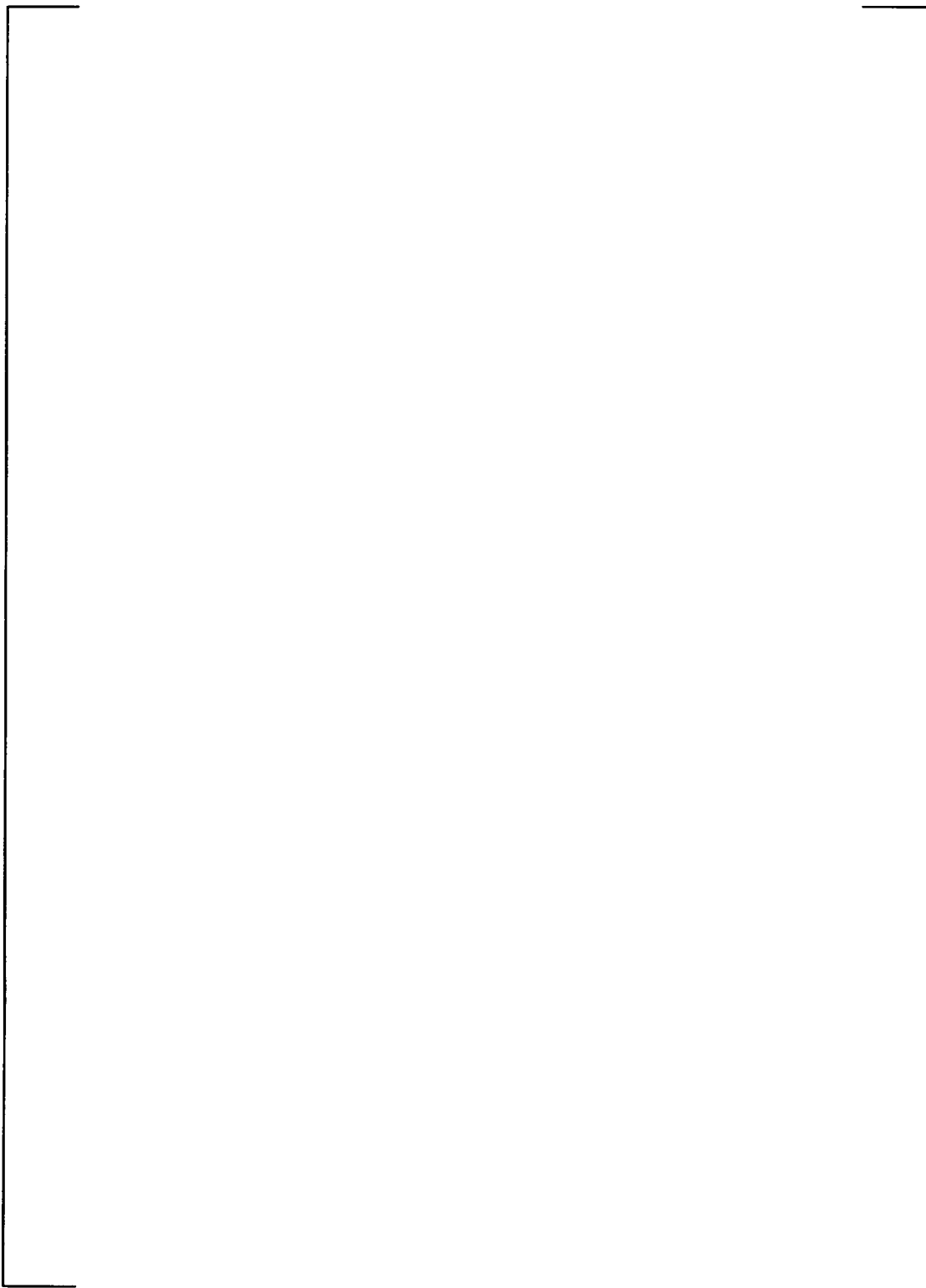


Figure 5-2
Tube Hydraulic Expansion Process Schematic

6.0 LEAK RATE EVALUATION

The primary-to-secondary leakage from through-wall cracks within the hydraulic expansion region in tubesheet would vary depending on [

] ^{a,c,e}. Normal operating leakage from throughwall cracks within the tubesheet is expected to be negligible. A number of both axial and circumferential cracks have been reported in the last several inspections of the Model F steam generators of the Callaway SGs. However, no significant primary-to-secondary leakage has been observed under normal operation. This experience is consistent with that of other model SGs for other types of expansion processes.

The leak rate evaluation to justify a partial length RPC inspection for the tubesheet region is based on a combination of [

] ^{a,c,e} is discussed in Section 6.1. Section 6.2 describes the leak rate calculation methodology. Section 6.3 presents results from the leakage evaluation.

6.1 TUBESHEET CONSTRAINING EFFECT ON CRACK OPENING

A test program carried out in support of an alternate repair criteria for another model SG (Reference 8.2) has shown that the [

] ^{a,c,e} are provided in Section 7.0 for applicable operating conditions.

The [

] ^{a,c,e}.

6.2 LEAK RATE ANALYSIS METHODOLOGY

The methodology used to calculate leakage is similar to that developed for previous alternate repair criteria. Leak rate from a flawed tube is determined by taking into account the flow resistances of both

the [

] ^{a.c.e.}.

The combined crack and tubesheet crevice flow calculation is performed using the Westinghouse proprietary code DENTFLO. The application of the DENTFLO Code requires the input of a [

The effective length is used as input to the DENTFLO code.] ^{a.c.e.}

6.3 LEAK RATE RESULTS

The steam line break (SLB) conditions provide the [

] ^{a.c.e.}. Therefore, accident condition leak rates in this evaluation are calculated with the SLB primary-to-secondary pressure differential.

Leakage through the tubesheet crevice around a tube postulated to contain a flaw within the tubesheet was calculated considering both [] ^{a.c.e.}. The calculations were performed

for cracks located at different depths [

] a.c.e.

7.0 STRUCTURAL ANALYSIS

An evaluation was performed to determine the contact pressures between the tubes and tubesheet in the Callaway steam generators as part of the H* analysis. The evaluation utilized [

] ^{a,c,e}, were determined.

The same contact pressure results were used [

] ^{a,c,e} were also included.

Because the P* analysis postulates that a [

] ^{a,c,e} for determination

of P*.

7.1 EVALUATION OF TUBESHEET DEFLECTION EFFECTS FOR H* AND H* LEAKAGE

A finite element model developed previously for the Model F channelhead/tubesheet/shell region was used to determine the tubesheet hole dilations in the Callaway steam generators. [

] ^{a,c,e} loads in the tube.

7.1.1 Material Properties and Tubesheet Equivalent Properties

The material of construction for the tubing in the steam generators is a nickel base alloy, Alloy 600, most of the tubes in a mill annealed condition and the remainder in the thermally treated (TT) condition. Summaries of the applicable mechanical and thermal properties for the tube material are provided in Table 7.1-1. The tubesheet material is SA-508, Class 2a, and its properties are in Table 7.1-2. The shell material is SA-533 Grade A Class 2, and its properties are in Table 7.1-3. The channelhead material is SA-216 Grade WCC, and its properties are in Table 7.1-4. The material properties are from Reference 8.4.

The perforated tubesheet in the Model F channelhead complex is treated [

] ^{a,c,e} in the perforated region of the tubesheet for the finite element model. The material properties of the tubes are not utilized in the finite element model, but are listed in Table 7.1-1 for use in the calculations of the tube/tubesheet contact pressures.

a.c.e

These data were fit to the polynomial below:

[

] a.c.e

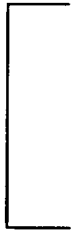
[]^{a,c,e}

The radial expansion of the hole I.D. is given by:

[

]^{a,c,e}

The resulting equation is:



a.c.e

For a given set of primary and secondary side pressures and temperatures, the above equation is solved for selected elevations in the tubesheet to obtain the contact pressures between the tube and tubesheet as a function of radius. The elevations selected ranged from [

]a.c.e

7.1.3 Callaway Contact Pressures

7.1.3.1 Normal Operating Conditions

The loadings considered in the analysis are based on an umbrella set of conditions as defined in References 8.8, 8.9 and 8.10. The current operating parameters from Reference 8.10 are used. The temperatures and pressures for normal operating conditions at Callaway are therefore:

	Case 2 ⁽¹⁾	Case 3 ⁽²⁾
Primary Pressure	= 2235 psig	2235 psig
Secondary Pressure	= 893 psig	955 psig
Primary Fluid Temperature (T _{hot})	= 615.3 °F	620.0 °F
Primary Fluid Temperature (T _{cold})	= 551.3 °F	556.6 °F
Secondary Fluid Temperature	= 533.0 °F	540.8°F

(1) Minimum Steam Temperature and Pressure in Reference 8.10

(2) Maximum Steam Temperature and Pressure in Reference 8.10

The primary pressure [

] ^{a.c.e.}

7.1.3.2 Faulted Conditions

The following conservative initial conditions and assumptions apply to the analyses of SG faulted conditions:

- One occurrence per plant lifetime.
- The initial conditions for the transient start with the plant operating at full power.
- The fault rupture is located outside of containment, so that secondary side coolant expulsion challenges the site radiological limits.
- The accident causes an immediate reactor trip and actuation of the Safety Injection System.

- Off-site power is lost at the beginning of the transient, causing all reactor coolant pumps to be de-energized, so that primary coolant flow coasts down to the natural circulation rate.
- The Safety Injection System operates at design capacity and repressurizes the Reactor Coolant System within a relatively short time.

The analyses of this hypothetical transient incorporates [

] ^{a,c,e} cases are considered in this section.

7.1.3.2.1 Feedline Break

The temperatures and pressures for Feedline Break, using the guidelines from Reference 8.9, are:

	Case 2 ⁽¹⁾	Case 3 ⁽²⁾
Primary Pressure	= 2650 psig	2650 psig
Secondary Pressure	= 0 psig	0 psig
Primary Fluid Temperature (Thot)	= 591.3 °F	596.0 °F
Secondary Fluid Temperature	= 533.0 °F	540.8 °F

(1) Minimum Steam Temperature and Pressure in Reference 8.9

(2) Maximum Steam Temperature and Pressure in Reference 8.9

The Feedline Break condition [

] ^{a,c,e}.

7.1.3.2.2 Steam Line Break

The Steam Line Break starts from hot standby conditions. As a result of SLB, [

] the hot leg and cold leg.

7.1.4 Summary of Results

For Callaway, the contact pressures between the tube and tubesheet are plotted versus radius in Figures 7.2-2a through and 7.2-3b. Results from these figures are summarized in Table 7.2-1a and 7.2-1b.

7.2 DETERMINATION OF TUBE-TO-TUBESHEET CONTACT PRESSURE FOR H*

The H* partial-length RPC justification relies on knowledge of [


] ^{a.c.e}

For the tube anchorage effect, it is necessary to demonstrate that the [

] ^{a.c.e}.

The thickness of the test block used in the pullout tests of Reference 9.28 was 25.24 inches. Assuming that the pull out force is evenly distributed along the length of the tube in contact with the tubesheet results in a minimum resistance to pull out of [

a.c.c



so that,



j.a.c.e.

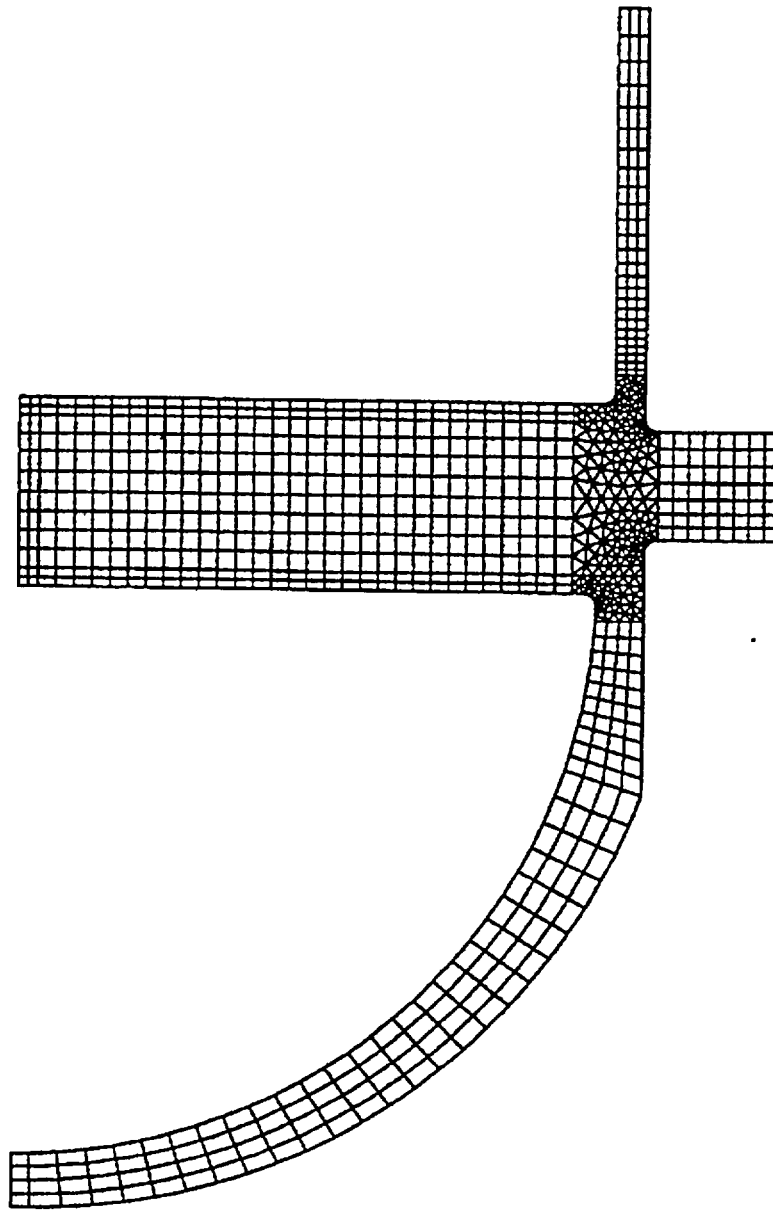


Figure 7-1
Finite Element Model of Model F Tubesheet Region

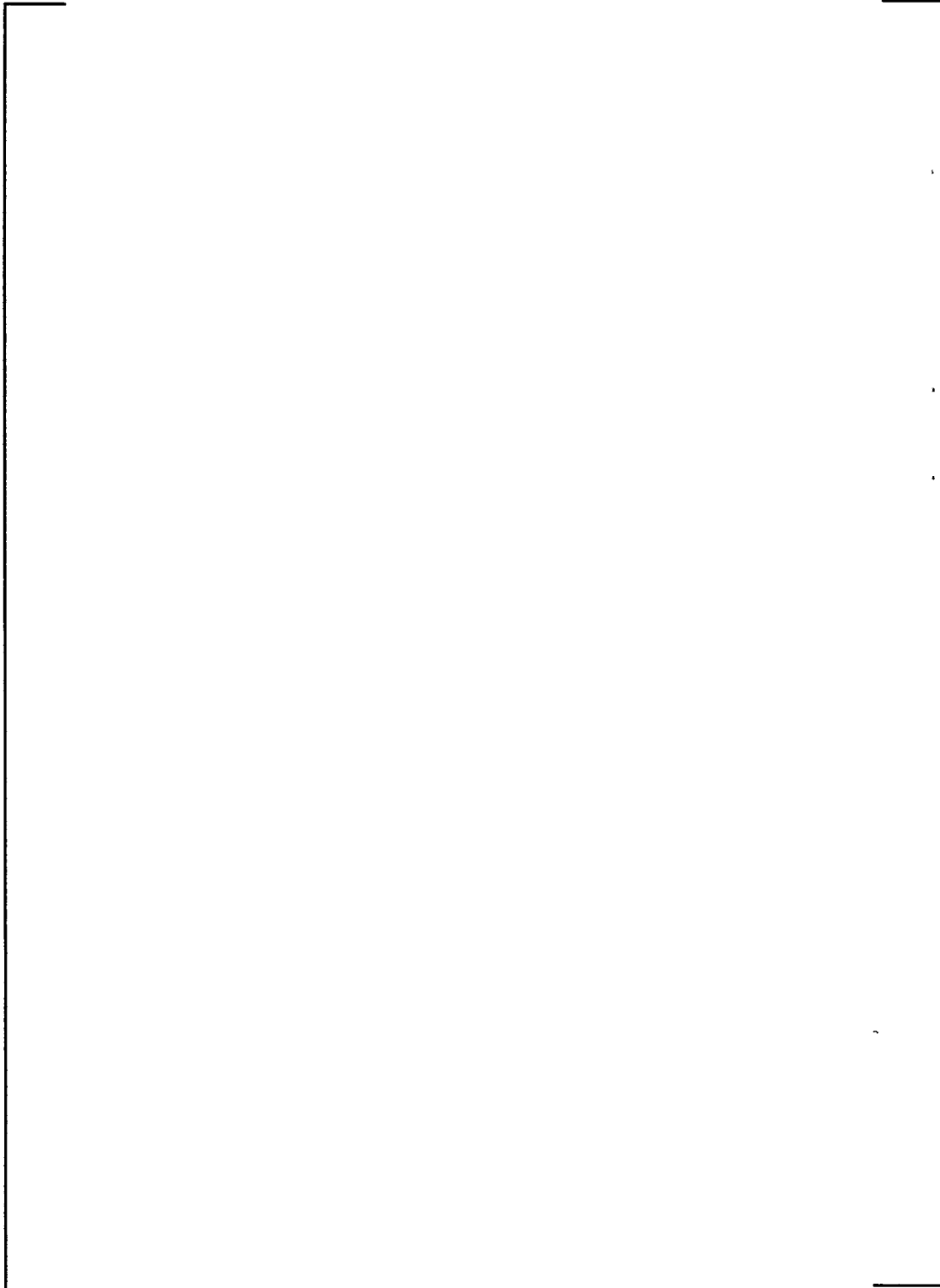


Figure 7.2-2a
Contact Pressures for Normal Condition at Callaway, Psec = 893 psig

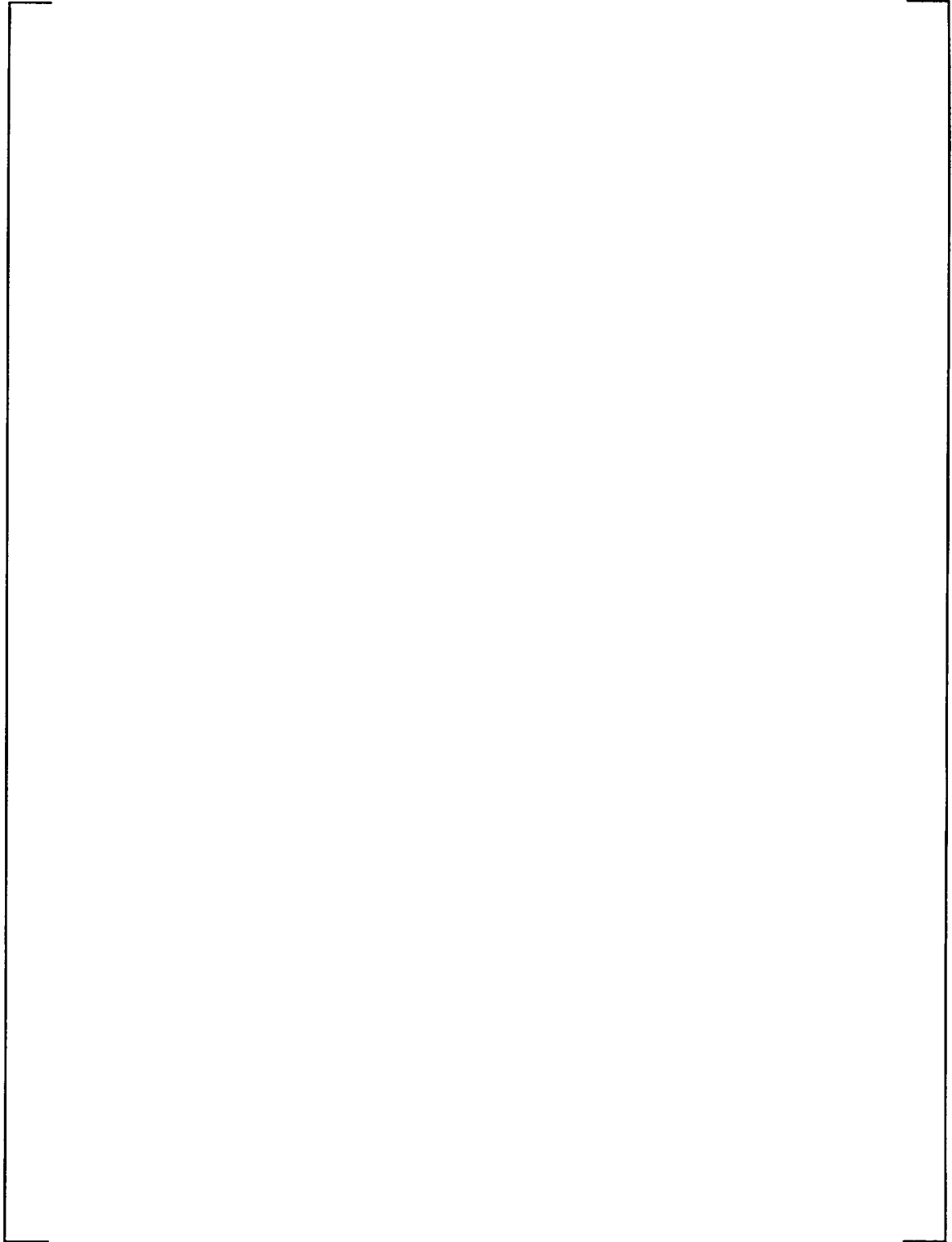


Figure 7.2-2b
Contact Pressures for Normal Condition at Callaway, Psec = 955 psig

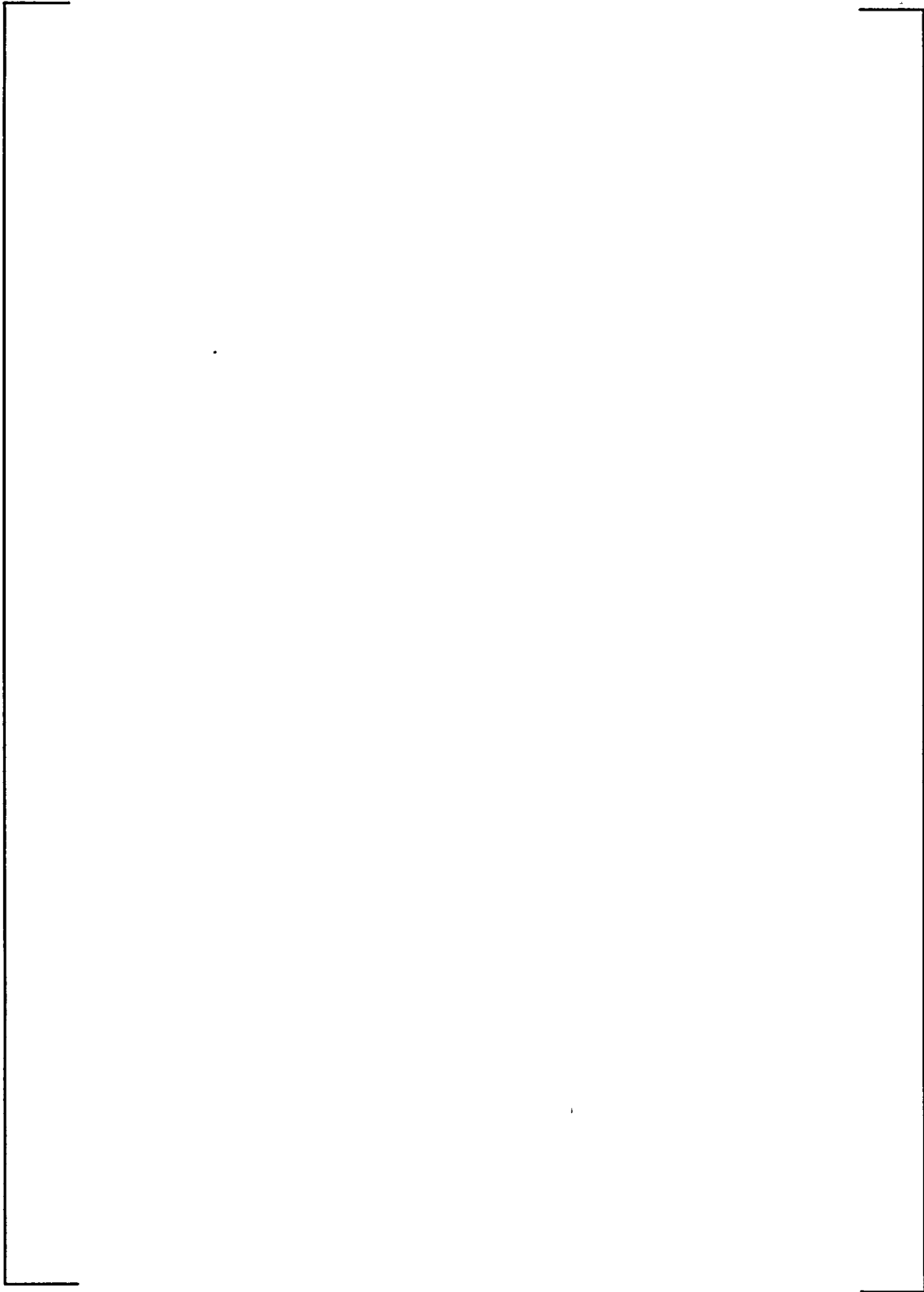


Figure 7.2-3a
Contact Pressures for FLB and SLB Conditions at Callaway, Tsec = 533.0 °F

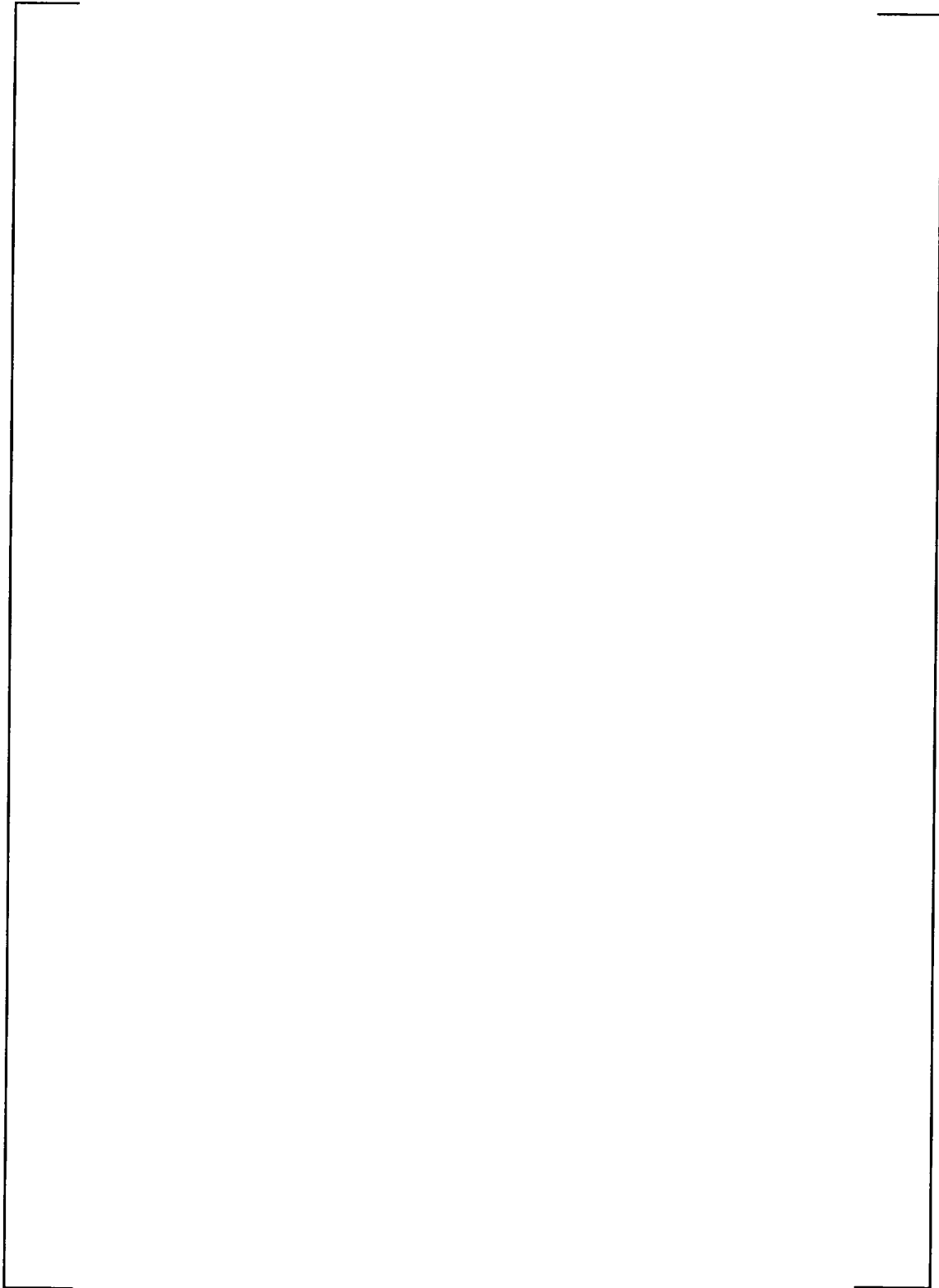


Figure 7.2-3b
Contact Pressures for FLB and SLB Conditions at Callaway,
Tsec = 540.8 °F

**Table 7.1-1
Summary of Material Properties
Alloy 600 Tube Material**

PROPERTY	TEMPERATURE (°F)						
	70	200	300	400	500	600	700
Young's Modulus psi x 1.0 E06	31.00	30.20	29.90	29.50	29.00	28.70	28.20
Coefficient of Thermal Expansion in/in/°F x 1.0 E-06	6.90	7.20	7.40	7.57	7.70	7.82	7.94
Density lb-sec ² /in ⁴ x 1.0E-04	7.94	7.92	7.90	7.89	7.87	7.85	7.83
Thermal Conductivity Btu/sec-in-°F x 1.0E-04	2.01	2.11	2.22	2.34	2.45	2.57	2.68
Specific Heat Btu-in/lb-sec ² -°F	41.2	42.6	43.9	44.9	45.6	47.0	47.9

Table 7.1-2
Summary of Material Properties
SA-508 Class 2a Tubesheet Material

PROPERTY	TEMPERATURE (°F)						
	70	200	300	400	500	600	700
Young's Modulus psi x 1.0 E06	29.20	28.50	28.00	27.40	27.00	26.40	25.30
Coefficient of Thermal Expansion in/in/°F x 1.0 E-06	6.50	6.67	6.87	7.07	7.25	7.42	7.59
Density lb-sec ² /in ⁴ x 1.0E-04	7.32	7.30	7.29	7.27	7.26	7.24	7.22
Thermal Conductivity Btu/sec-in-°F x 1.0E-04	5.49	5.56	5.53	5.46	5.35	5.19	5.02
Specific Heat Btu-in/lb-sec ² -°F	41.9	44.5	46.8	48.8	50.8	52.8	55.1

Table 7.1-3
Summary of Material Properties
SA-533 Grade A Class 2 Shell Material

PROPERTY	TEMPERATURE (°F)						
	70	200	300	400	500	600	700
Young's Modulus psi x 1.0 E06	29.20	28.50	28.00	27.40	27.00	26.40	25.30
Coefficient of Thermal Expansion in/in/°F x 1.0 E-06	7.06	7.25	7.43	7.58	7.70	7.83	7.94
Density lb-sec ² /in ⁴ x 1.0E-04	7.32	7.30	7.283	7.265	7.248	7.23	7.211

Table 7.1-4
Summary of Material Properties
SA-216 Grade WCC Channelhead Material

PROPERTY	TEMPERATURE (°F)						
	70	200	300	400	500	600	700
Young's Modulus psi x 1.0 E06	29.50	28.80	28.30	27.70	27.30	26.70	25.50
Coefficient of Thermal Expansion in/in/°F x 1.0 E-06	5.53	5.89	6.26	6.61	6.91	7.17	7.41
Density lb-sec ² /in ⁴ x 1.0E-04	7.32	7.30	7.29	7.27	7.26	7.24	7.22

Table 7.2-1a
Maximum/Minimum Contact Pressures between the Tube and Tubesheet
Including End Cap (Axial) Load on Tube

At Callaway with Psec = 893 psig

a.c.e



Table 7.2-1b
Maximum/Minimum Contact Pressures between the Tube and Tubesheet
Including End Cap (Axial) Load on Tube
At Callaway with Psec = 955 psig

a.c.e



Table 7.2-2a
Cumulative Forces Resisting Pull Out from the Top of the Tubesheet
Callaway – Hot Leg Normal Conditions – Axial Load Included, Psec = 893 psig

Variation of Contact Pressures through Tubesheet

a.c.e



Table 7.2-2b
Cumulative Forces Resisting Pull Out from the Top of the Tubesheet
Callaway – Hot Leg Normal Conditions – Axial Load Included, Psec = 955 psig

Variation of Contact Pressures through Tubesheet

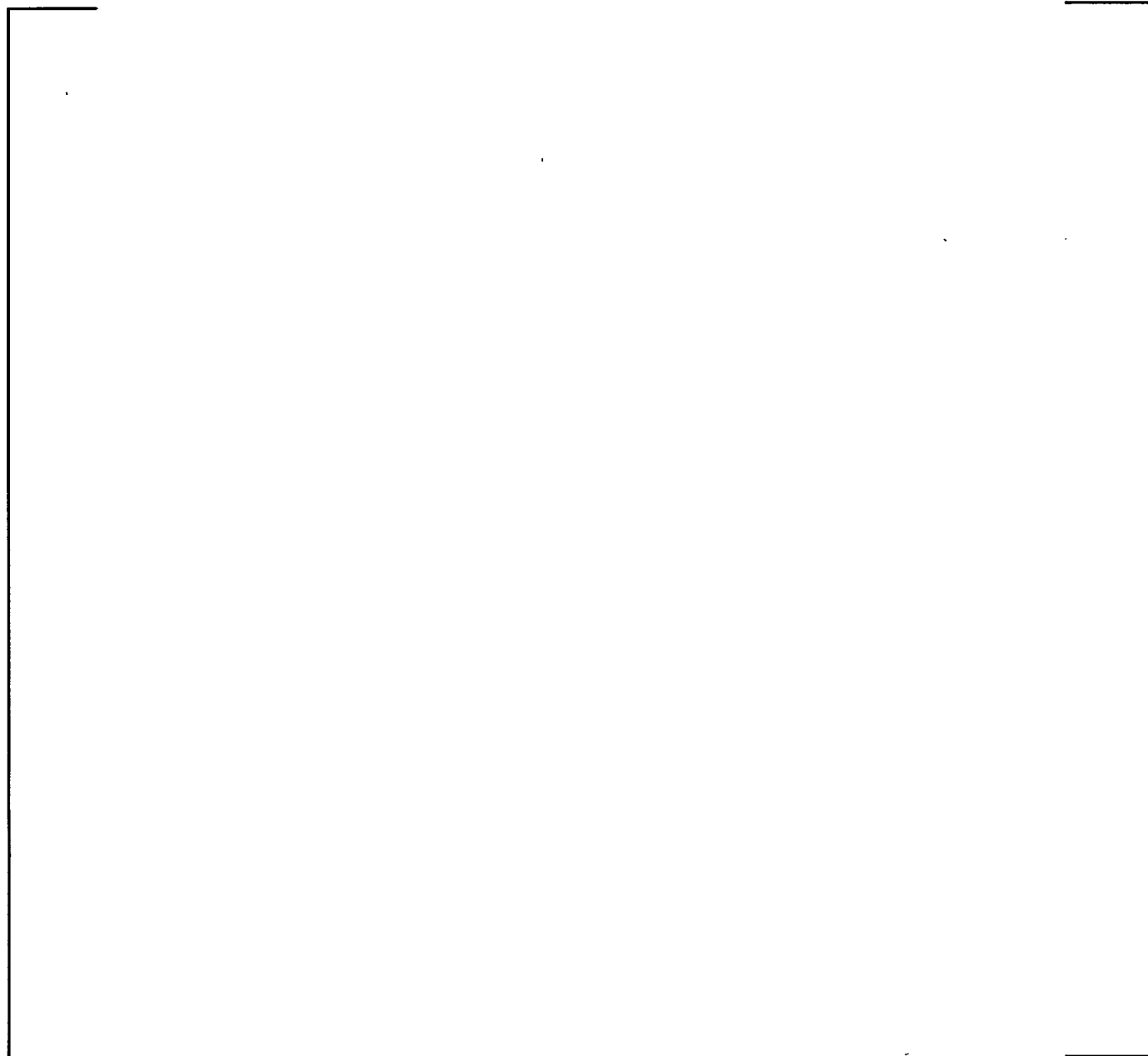
a,c,e



Table 7.2-3
Cumulative Forces Resisting Pull Out from the Top of the Tubesheet
Callaway Faulted (SLB) Conditions – Axial Load Included

Variation of Contact Pressures through Tubesheet

a,c,c



7.3 RESISTANCE TO PULLOUT – P*

P* theory assumes that a tube, which is postulated to become fully separated below the secondary face of the tubesheet, will be retained within the tubesheet, because the resulting primary to secondary pressure differential (ΔP) vertical thrust from the separated tube leg will be reacted and supported by the next row (outboard) adjacent tube. The maximum upward displacement of the separated tube end plus at least ¼ inch (to retain the separated tube end in the tubesheet hole) is required to determine P*. This upward displacement is calculated using various finite element (FE) models of the separated tubes and row adjacent supporting tubes as described in this section for the overall maximum ΔP load. Based on these calculations, P* is less than []^{a,c,e} inches for all locations in the tube bundle that have an outer next row, both hot leg and cold leg. In addition, the calculated stresses in the supporting tubes are shown to satisfy the structural criteria of the ASME Code, Reference 8.4 for the ΔP loads specified in References 8.8 and 8.9.

7.3.1 Major Assumptions

The major assumptions made in the P* analysis concern U-bend out-of-plane effects, dynamic effects and the selection of representative locations in the Model F tube bundle for evaluation.

U-bend Out-of-Plane Effects

The extrados of the separated tube will initially strike the intrados of the row-adjacent intact tube. [

] ^{a,c,e}.

Figure 7.3-3 is a typical cross-section, [

] ^{a,c,e}.

The elastic strain energy required to establish the snap through mode shapes may be calculated using the 3D FE pipe models of the tubes discussed in Section 7.3.5. The minimum strain energy occurs for the largest (most-flexible) U-bend radii, Rows 57, 58 and 59. The initial contact for Row 58 is calculated to occur at node 84 near node 85 (see Section 7.3.6 and Table 7.3-7). Thus, it is conservative to assume snap through occurs only at nodes 85, 77 and 68. Figures 7.3-4A and 4B show the resulting FE deformed geometry plots for this case. The resulting FE calculated elastic strain energy is over [] ^{a,c,e}

Actually, the total strain energy would be significantly higher than []^{a,c,e} since the bending stresses in the separated tube greatly exceed yield resulting in plastic flow-work, which is unaccounted for in the elastic solution. Also unaccounted for are the torsion strain energy and the energy lost to sliding friction at the tube-TSP, tube-AVB and tube-tube contacts.

The maximum kinetic energy of the Row 58 separated tube (at impact with Row 59) is about []^{a,c,e}, as calculated in Section 7.3.6 and listed in Table 7.3-9. Actually, the kinetic energy available at impact would be less (than []^{a,c,e}) since the effects of sliding friction and strain energy of the separated tube in bending have been neglected. It is unlikely that sufficient energy is available to cause out-of-plane snap through, even at Row 58, the most flexible separated tube location. Therefore, it is assumed that the separated and intact tubes remain essentially in-plane after contact, and that out-of-plane effects are limited to considering the stresses in the supporting intact tube due to the out-of-plane contact forces, shown in Figure 7.3-1.

Dynamic Effects

The separated tube has kinetic energy when it strikes the intact tube, and it is necessary to consider dynamic amplification of the separated tube displacement for the P* calculation. Because of the complex nonlinear nature of the surface-to-surface contact, such effects are best simulated assuming []^{a,c,e}, as shown in Figure 7.3-6 and as discussed in Section 7.3.5.

Thermal Effects

It is reasonable to assume that the average temperatures of two active row adjacent tubes (i.e., in the same column) are essentially []^{a,c,e}. Further, it is conservative to assume the material properties and structural strengths are evaluated at the []^{a,c,e}. Thus, P* analysis results apply to either the hot leg or cold leg.

Tube Rows Selected for P* Evaluation

In order to cover the tube bundle, Rows 4/5, Rows 30/31 and Rows 58/59 are selected for the P* evaluation. The small radius rows (4/5) have []^{a,c,e}, but are relatively stiff in both in-plane and out-of-plane bending. The largest P* radius combination is Rows 58/59, which are very flexible in bending and have []^{a,c,e}, as shown in Figure 7.3-2. Rows 30/31 are assumed to have []^{a,c,e} and represent the middle of the tube bundle. In addition, Row 57, which []^{a,c,e}, is considered in the out-of-plane energy analysis, as discussed above.

7.3.2 Loads

P* requires that the next row-adjacent tube provide support for a postulated fully separated tube inside the tubesheet. P* is the maximum lift-distance of the postulated separated tube at the secondary face of the tubesheet plus at least ¼ inch to assure the separated tube end remains in the tubesheet. Therefore, the maximum separated tube lift-distance should be calculated for the specified overall maximum primary-to-secondary pressure differential (ΔP) and should include dynamic amplification effects for a suddenly applied load.

The overall maximum pressure differential occurs for the []^{a,c,e} for a Model F plant, which is over []^{a,c,e} for Callaway. In addition, a dynamic amplification factor, which is as high as []^{a,c,e} (Table 7.3-10), is used giving a combined safety factor on the order of 3 with respect to the normal operation ΔP . This approach compares well to the static pullout load used for determination of H* based on 3 × normal operating ΔP , as required by RG 1.121. Finally, the next row-adjacent supporting tube must meet the rules in Section III, Subsection NB of the ASME Code, for all specified loading conditions, design, normal, upset, test, emergency and faulted

The load conditions, used in the P* analysis, are listed in Table 7.3-1. P* is determined by []^{a,c,e}. Again, the intact tube must meet the ASME Code structural criteria for all of the loading conditions specified in Table 7.3-1

7.3.3 Material Properties

Table 7.3-2 lists the material properties used for the SB-163 TT Alloy 600 tube material in the P* analysis. All properties are conservatively taken at []^{a,c,e}.

7.3.4 Acceptance Criteria

The ASME Code stress intensity limits, used in the P* analysis, are listed in Table 7.3-3. These limits apply to the intact tube supporting the separated tube.

The maximum kinetic energy of the Row 58 separated tube (at impact with Row 59) is about []^{a,c,e}, as calculated in Section 7.3.6 and listed in Table 7.3-9. Again, the actual kinetic energy available at impact would be less (than []^{a,c,e}) since the effects of sliding friction and strain energy of the separated tube in bending have been neglected. The local dynamic effects at impact may be evaluated by comparison with the kinetic energy of the []^{a,c,e}

From page 2-48 of Reference 8.12, the puncture kinetic energy was estimated to exceed []^{a,c,e}. Therefore, based on both the energy level required for local fracture and the more favorable geometries of the impacting surfaces, no deleterious local effects are expected due to the impact of the postulated separated tube's extrados with the intact tube's intrados in the P* model

Since the tubes are ductile, the limits in Table 7.3-3 are applied to stresses calculated statically for the load conditions listed in Table 7.3-1. Thus, no shock factors are required in the stress evaluation since

the peak dynamic loads act for a very small time period. However, dynamic amplification factors are employed to calculate the displacements for P* as discussed in Section 7.3.6.

The fatigue usage factor due to P*, when added to the maximum fatigue usage factor calculated for a Model F tube in Reference 8.14, must not cause the combined overall usage factor to exceed the ASME Code limit of one. At most, the P* stress range for cycling loading is assumed to occur []^{a,c,e}. Since the limit on the upset range is 3S_m, the maximum amplitude would be 1.5S_m or 39.9 ksi. Conservatively assuming a maximum stress riser of 2, returns the peak stress to 79.8, say 80 ksi. From the fatigue design curve in Reference 8.4 for Alloy 600, the allowable cycles are over 4000, giving at most an additional usage factor of []^{a,c,e}. From Table 1-1 of Reference 8.14, the maximum cumulative usage factor in the Model F U-bend region is only about []^{a,c,e}. Thus, any additional fatigue usage due to P* is negligible.

7.3.5 Finite Element Models

The displacements of the separated tubes and row adjacent supporting tubes are calculated using the FE models described below.

Static Models

The separated and intact tubes are modeled using []

[]^{a,c,e}. Dynamic effects are considered using amplification factors obtained with the dynamic models, as discussed below.

Figures 7.3-5A, 5B and 5C show details of the []^{a,c,e}, which are typical for the simulation of Rows 4/5, 30/31 and 58/59. Table 7.3-4 lists the geometric parameters used to develop the 3D pipe element models. The tube support plates (TSPs) are assumed to []

[]^{a,c,e}.

Dynamic Models

The separated tube has kinetic energy when it strikes the intact tube, and it is necessary to consider dynamic amplification of the separated tube displacement for the P* calculation. []

[]^{a,c,e}

[

]a.c.e.

7.3.6 Displacement Results

The maximum displacement results at the selected tube row combination locations in the bundle are required to calculate P^* . In turn, this requires simulation of the [

]a.c.e.

Initial Surface-to-Surface Contact

Figure 7.3-7 shows schematically the geometric logic employed to calculate the upward displacement of the tangent point A due to initial surface-to-surface contact. [

]a.c.e.

[

$\delta^{a,c,e}$. The resulting tangent point lift from A to A' is also the vertical upward displacement of the separated tube straight leg at top of the tubesheet due to the initial surface-to-surface contact.

Subsequent Point-to-Point Contact

The subsequent displacements due to point-to-point contact are [

$\delta^{a,c,e}$. These are added to the initial surface-to-surface results (from Table 7.3-7) to give the combined statically calculated displacements of the separated tube at the top of the tubesheet, also listed in Table 7.3-8. These combined static results are increased for dynamic effects as discussed next.

Dynamic Amplification

Prior to performing FE time-history solutions using the [

$\delta^{a,c,e}$

[

] ^{a,c,e}. At impact, the maximum kinetic energy for Row 58 is about [] ^{a,c,e} for an impact velocity of [] ^{a,c,e}. (Note: The use of the term δ in this section is unrelated to the use of it in another section of this report.)

The dynamic displacement amplification factor (λ) is defined as [

] ^{a,c,e}.

7.3.7 Structural Evaluation Results

Primary Membrane Stress Evaluation

The P* primary stress evaluation of the intact tube conservatively neglects the remaining intact leg of the separated tube and assumes that all of the resulting pressure differential thrust from the separated tube leg is carried equally by each leg of the row adjacent intact tube. Table 7.3-11 lists the resulting calculated axial primary stresses in the intact tube straight legs for the specified Model F load conditions. Table 7.3-12 shows the P* primary stress evaluation, which considers the combined total axial stress from Table 7.3-11, the hoop stress due to the primary to secondary ΔP , the radial stress, and the resulting primary membrane stress intensity P_m . Minimum tube cross section properties are employed to calculate the primary stresses. [

] ^{a,c,e}.

As seen in Table 7.3-12, the ratio of P_m to the allowable stress intensity is less than one for all specified load conditions indicating that the ASME Code primary stress limits are satisfied for the intact tube.

Out-of-Plane Load Cases

It is assumed that out-of-plane effects are limited to considering the stress (mostly bending) in the supporting intact tubes due to the out-of-plane contact forces, i.e., the H component of the contact force N, shown in Figure 7.3-1. The vertical component (V) of the contact force N is the compression force in the contact elements obtained from the FE models considering in-plane loading only. The resulting out-of-plane horizontal force (H), acting in opposite directions on the separated and intact tubes, is obtained using the geometric relationship shown in Figure 7.3-1. This relationship depends on [] ^{a,c,e}

[

] ^{a,c,e}.

Using the above conservative misalignment assumptions and the in-plane 1st pass results that calculate the vertical contact forces (V) it is possible to determine the resulting out of plane forces (H) at each contact point between the separated and intact tubes. These H reactions are applied as equal and opposite FZ forces on the end nodes defining the contact elements shown in Figure 7.3-5B. Note that some of the gaps are open, and there is no contact (V = 0) and there is no out-of-plane force (H = 0). In of the each in-plane (pass 1) and out-of-plane (pass 2) 3D pipe element models, four load steps are used corresponding to the design (or test), upset, emergency and faulted loads listed in Table 7.3-5. The resulting 2nd pass stresses in the intact tube are used to evaluate the bending stresses as discussed below.

Primary Membrane plus Bending Stress Evaluation

In most bundle locations, the P* bending stresses, due to both in-plane and out-of-plane loads, occur in the [

] ^{a,c,e}. The overall maximum in-plane plus

out-of-plane stresses result from the [

] ^{a,c,e}. Assuming the overall worst case minimum cross-sectional properties for primary loading (see Tables 7.3-11 and 12), [

] ^{a,c,e}. The resulting primary plus secondary stress intensity for the FLB load is $P_m + P_b = [$

] ^{a,c,e} all primary plus bending stress limits for the Row 59 intact tube, due to out-of-plane loads, are satisfied with positive structural margins. Since the margins are substantial, significantly larger tube misalignments at contact (than the assumed [] ^{a,c,e} could be tolerated.

Secondary Stress Evaluation

The P* bending stresses in the intact tube are []^{a,c,e}. There are no secondary stress limits for the emergency and faulted load conditions. The overall maximum bending stresses occur in the [

] ^{a,c,e}. The resulting maximum primary plus secondary stress intensity range is 35 ksi, which is less than the $3S_m$ allowable of 79.8 ksi, indicating that the ASME Code secondary stress limits are satisfied.

**Table 7.3-1
Model F Primary to Secondary ΔP Loads Used in P* Analysis**

ASME Code Classification	P_p Primary Side Pressure (psia)	P_s Secondary Side Pressure (psia)	$\Delta P = P_p - P_s$ Primary to Secondary Pressure Differential (psi)	Reference
Design	[] ^{a,c,e}	Reference 8.8
Max-Upset	[] ^{a,c,e}	Table K-30 of Reference 8.15
Test	[] ^{a,c,e}	Limited to Design ΔP by Section XI (IWA 4700, IWA 500, IWB 5000), Reference 8.11.
Emergency	[] ^{a,c,e}	Small Steam Line Break, Systems Standard 1.3F, Reference 8.9
Faulted	[] ^{a,c,e}	Feed Line Break, Systems Standard 1.3F, Reference 8.9

**Table 7.3-2
Material Properties Used in P* Analysis**

Property	Value [] ^{a,c,e}	Reference
Elastic Modulus	28.45×10^6 psi	Table I-6.0 of Reference 8.4
Thermal Expansion Coefficient	7.9×10^{-6} °F ⁻¹	Table I-5.0 of Reference 8.4
Poisson's Ratio	0.3	Assumed
Metal Weight Density	0.307 lbf/in ³	Page 4-9 of Reference 8.14
Effective Mass Density*	0.001076 lbf-sec ² /in ⁴	Page 4-10 of Reference 8.14
S_m Primary Membrane Limit	26.6 ksi	Table 6-1 of Reference 8.14
S_y Yield Strength	35.2 ksi	Table 6-1 of Reference 8.14
S_u Ultimate Tensile Strength	80.0 ksi	Table 6-1 of Reference 8.14

* Used in dynamic analysis and includes metal, internal water and external hydrodynamic masses based on the nominal cross section area of a Model F tube.

**Table 7.3-3
Stress Intensity Limits Used in P* Analysis**

ASME Code Classification	Basis for Stress Intensity Limit	P _m Limit (ksi)	P _m + P _b Limit* (ksi)	P _m + P _b + Q Limit (ksi)
Design	S _m	26.6	35.6	N/A
Upset	3S _m	N/A	N/A	79.8
Test	0.9S _y	31.7	42.5	N/A
Emergency	S _y	35.2	47.2	N/A
Faulted	0.7S _u	56.0	75.0	N/A

* Using a shape factor of 1.34 for the Model F tube.

Table 7.3-4

[

] ^{a,c,e}

Tube Row	U-bend Radius (inch)	Straight Leg* (inch)	[] ^{a,c,e}					
			# 1	# 2	# 3	# 4	# 5	# 6
4	[] ^{a,c,e}
5	[] ^{a,c,e}
30	[] ^{a,c,e}
31	[] ^{a,c,e}
57	[] ^{a,c,e}
58	[] ^{a,c,e}
59	[] ^{a,c,e}

* Straight leg length is from the top of the tubesheet to U-bend tangent.

Table 7.3-5
Vertical Forces Acting on Separated Tube Leg
Applied in P* FE Models (See Figures 7.3-5A, 5B and 5C)

Load Condition	ΔP (psi)	F_1 = Force on Tube Expansion (lbf)	F_{65} = Force at Tangent to U-bend (lbf)	Total Vertical Force (lbf)
Design or Test	[] ^{a,c,e}
Upset	[] ^{a,c,e}
Emergency	[] ^{a,c,e}
Faulted	[] ^{a,c,e}
Unit	[] ^{a,c,e}

Table 7.3-6

Tube Rows	Lump Masses ^A (lbf-sec ² /in)		Effective Spring Rates (lbf/in)		4% Damping Coefficient (lbf-sec/in)		Gap Stiffness (lbf/in)	Initial Gap ^B (inch)
	M_1	M_2	K_1	K_2	C_1	C_2		
4/5	[] ^{a,c,e}
30/31	[] ^{a,c,e}
58/59	[] ^{a,c,e}

A. Mass 1 is the separated tube, mass 2 is the next outer row-adjacent intact tube.

B. Initial gap is assumed to be UY_B vertical displacement at 1st contact from Table 7.3-7.

Table 7.3-7
Results of Initial Surface-to-Surface Contact Displacement Analysis

Tube Rows	1 st Node in FE Model to Contact (B)	θ Polar Angle to B (°)	ΔP_C Min ΔP For 1 st Contact (psi)	α Arc A'-B' Angle (°)	ϕ Solution Angle (°)	ψ Polar Angle to A' (°)	Tangent Lift (A to A') L + Yo (inch)	UY _B Vertical Disp at 1 st Contact (inch)
4/5	[] ^{a,c,e}
30/31	[] ^{a,c,e}
58/59	[] ^{a,c,e}

Table 7.3-8
Total Combined Static Surface-to-Surface and Point-to-Point Contact Displacement Analysis Results for the Separated Tube Straight Leg at the Top of the Tubesheet

Tube Rows	Point-to-Point FE Calculated Vertical Displacement at the Top of Tubesheet Due to FLB Load Applied Statically (inch)	Surface-to-Surface Tangent Lift (A to A') L + Yo from Table 7.3-7 (inch)	Total Combined Static Displacement at Top of Tubesheet (inch)
4/5	[] ^{a,c,e}
30/31	[] ^{a,c,e}
58/59	[] ^{a,c,e}

Table 7.3-9
Calculation of Maximum Kinetic Energy of Separated Tube at
Impact With Adjacent Intact Tube for []^{a,c,e}

Tube Rows	Separated Tube Mass M_1 (lbf-sec ² /in)	Initial Acceleration $A_o = F_{SLB} / M_1$ (in/sec ²)	δ_{GAP} Vertical Disp At 1 st Contact (inch)	V_c Contact Velocity (in/sec)	KE Kinetic Energy At 1 st Contact (in-lbf)	T_c Time to Initial Contact (sec)
4/5	[] ^{a,c,e}
30/31	[] ^{a,c,e}
58/59	[] ^{a,c,e}

Table 7.3-10
Dynamic Displacement Amplification Factors for []^{a,c,e}
Calculated Using []^{a,c,e} of Figure 7.3-6

Tube Rows	UY_D Maximum Dynamic Displacement Of Separated Tube (inch)	Time of Maximum Dynamic Displacement (second)	UY_S Maximum Static Displacement Of Separated Tube (inch)	$\lambda = UY_D / UY_S$ Dynamic Displacement Amplification Factor	$(UY_1)_S$ Total Combined Static Displacement at Top of Tubesheet from Table 7.3-8 (inch)	$(UY_1)_D = \lambda (UY_1)_S$ Maximum Dynamic Displacement at Top of Tubesheet (inch)
4/5	[] ^{a,c,e}
30/31	[] ^{a,c,e}
58/59	[] ^{a,c,e}

Table 7.3-11
Total Axial Primary Stress in Intact Tube Straight Legs
Model F Steam Generators

[

] ^{a,c,e}

Load Condition	P _p (psia)	P _s (psia)	ΔP = P _p - P _s (psi)	P _o Separated Tube Thrust (lbf)	Axial Stress Due to P _o (ksi)	Axial Stress Due to ΔP (ksi)	Total Axial Stress (ksi)
Design	[] ^{a,c,e}
Upset	[] ^{a,c,e}
Test	[] ^{a,c,e}
Emergency	[] ^{a,c,e}
Faulted	[] ^{a,c,e}

Table 7.3-12
P* Primary Stress Evaluation of Intact Tube
Model F Steam Generators

[

] ^{a,c,e}

Load Condition	ΔP (psi)	Total Axial Stress (ksi)	Hoop Stress Due to ΔP (ksi)	Radial Stress (ksi)	P _m Stress Intensity (ksi)	Allowable Intensity Stress (ksi)	Ratio P _m To Allowable
Design	[] ^{a,c,e}
Upset	[] ^{a,c,e}
Test	[] ^{a,c,e}
Emergency	[] ^{a,c,e}
Faulted	[] ^{a,c,e}

Figure 7.3-1
Schematic Showing Misalignment Between
Separated and Intact Tubes at Contact.

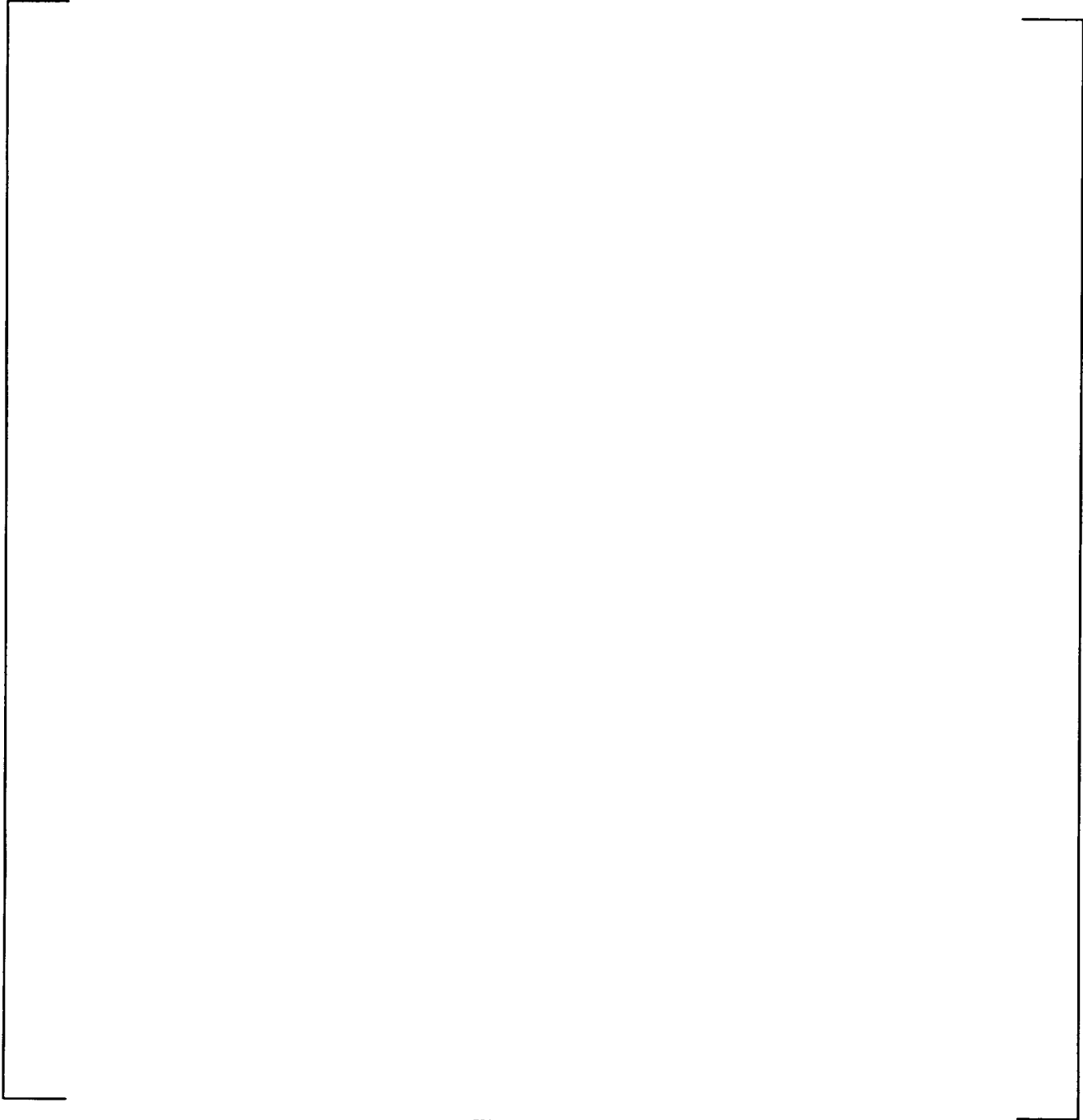


Figure 7.3-2
U-bend Region Showing AVBs and
Postulated Snap Through Mode Shape

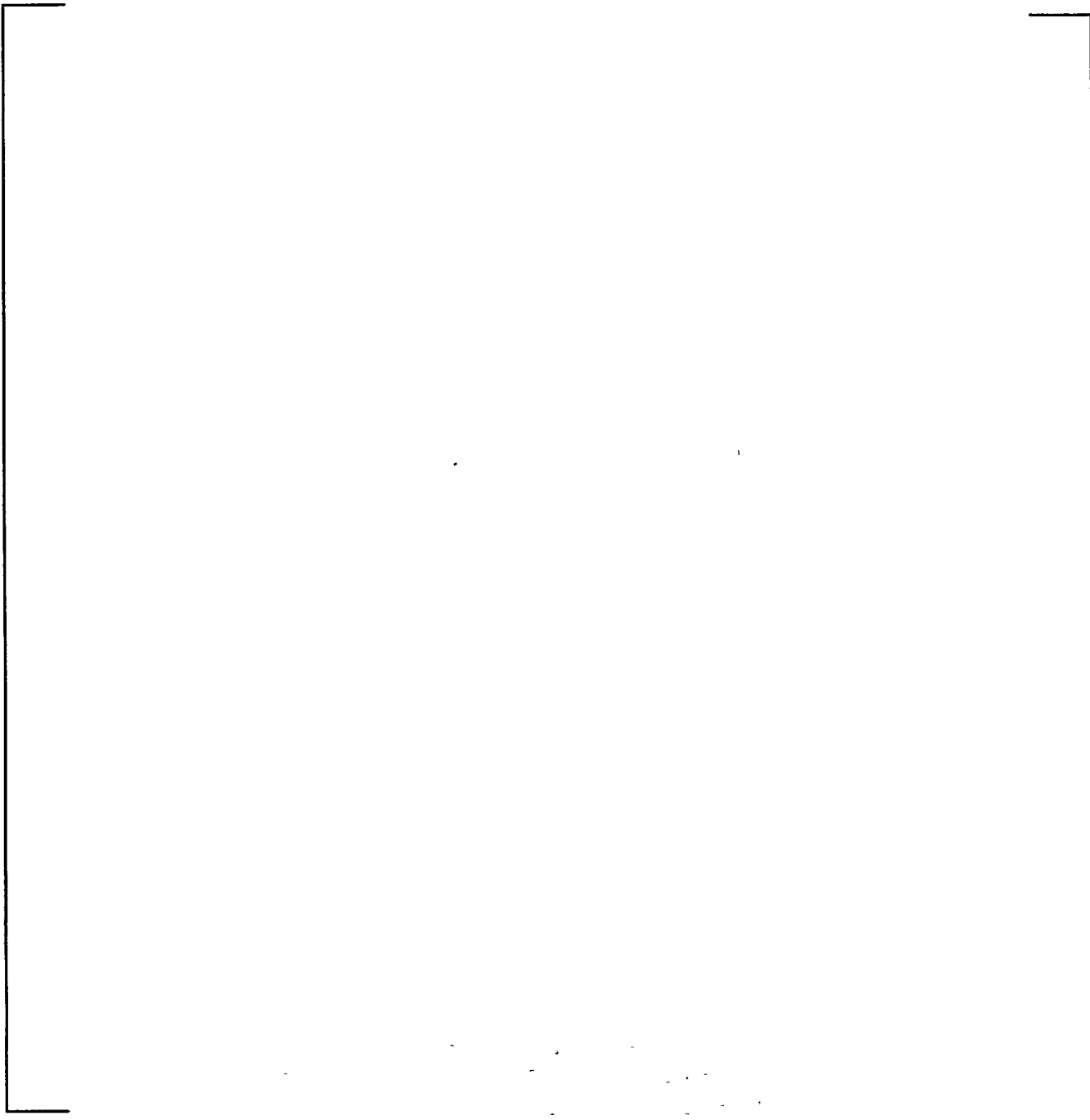


Figure 7.3.1-3
Minimum Required Out-of-Plane Motion Between AVB
Support Points for Postulated Snap Through



Figure 7.3-4A
In-Plane View FE Deformed Geometry Plot of Postulated
Snap Through at Nodes 68, 77 and 85 Used to Obtain
Minimum Strain Energy Required to Establish Snap Through

a.c.e



Figure 7.3-4B
Out-of Plane View FE Deformed Geometry Plot of Postulated
Partial Snap Through at Nodes 68, 77 and 85 Used to Obtain
Minimum Strain Energy Required to Establish Snap Through

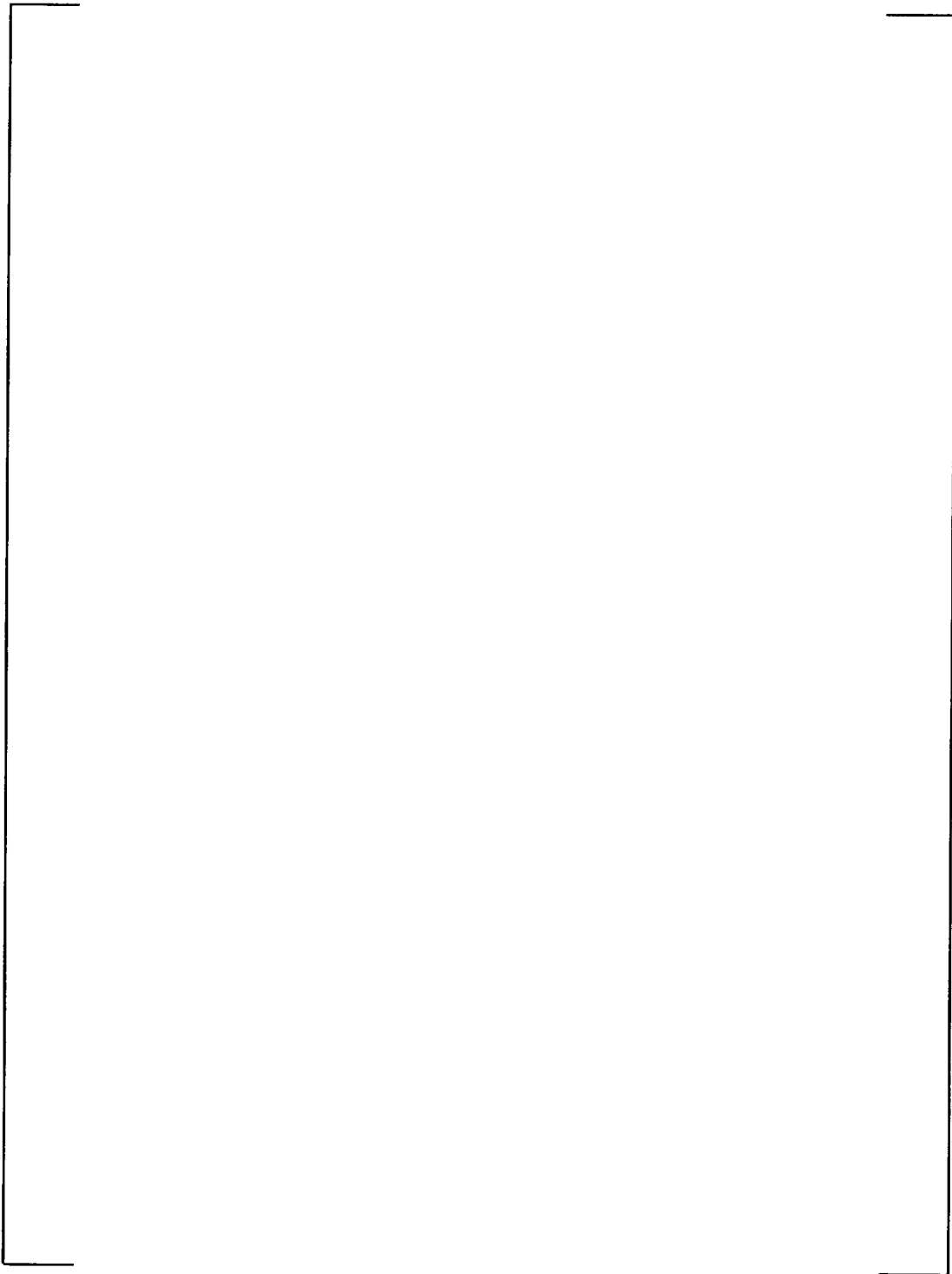


Figure 7.3-5A
FE Model – [

]a.c.e

a,c,e



Figure 7.3-5B
FE Model – [

]^{a,c,e}



Figure 7.3-5C
FE Model – [

]^{a,c,e}



Figure 7.3-6

[]
] a.c.e

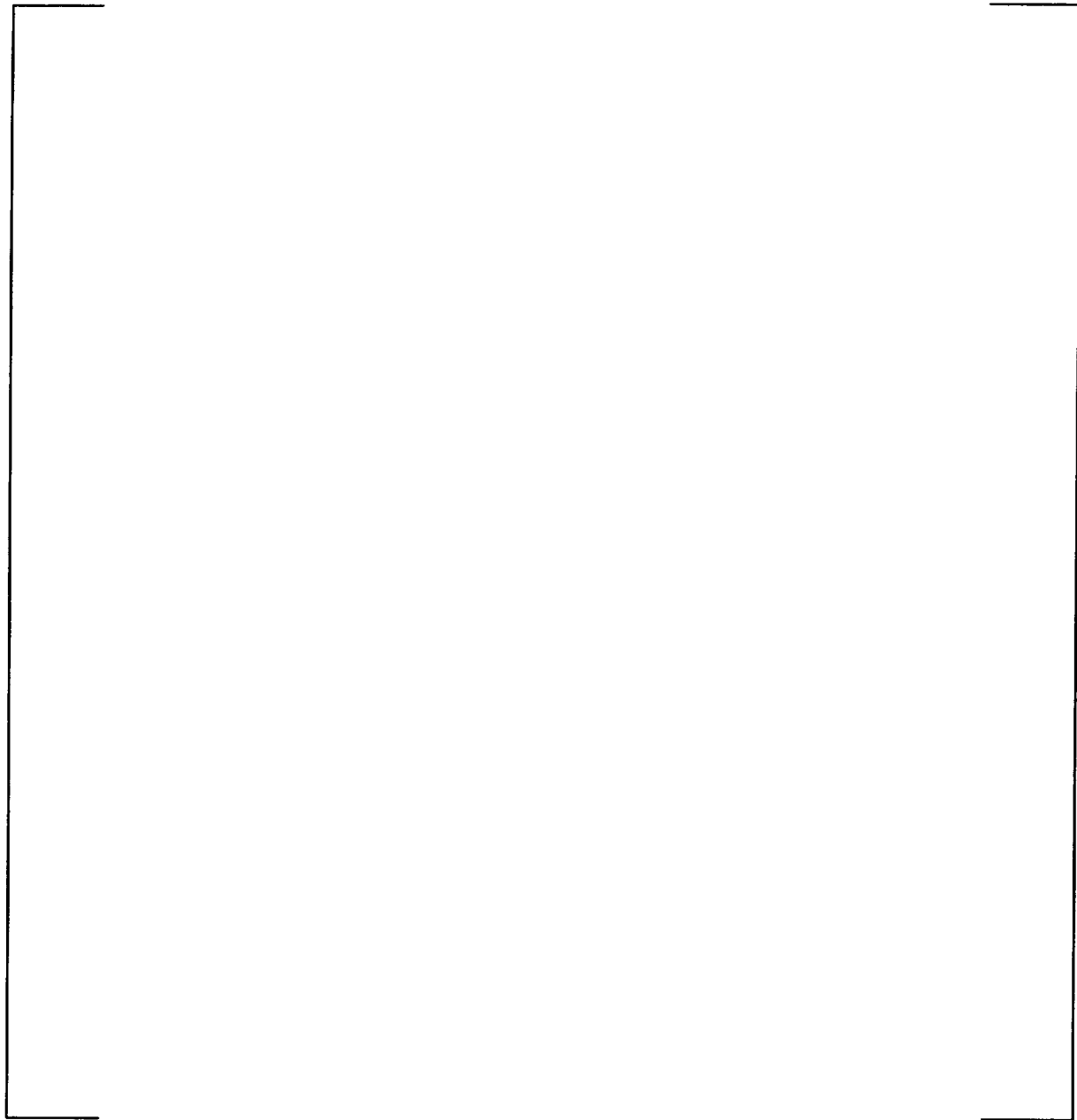


Figure 7.3-7
Geometry of Initial (1st) Surface-to-Surface Contact
Between Separated and Intact Tubes

[

] a,c,e



Figure 7.3-8
Static Point-to-Point In-plane Displacement Vectors
of Rows 4/5 U-bend Region Separated and
Intact Tubes For [

]^{a,c,e}



Figure 7.3-9
Static Point-to-Point In-plane Displacement Vectors
of Rows 30/31 U-bend Region Separated and
Intact Tubes For [

]a.c.e

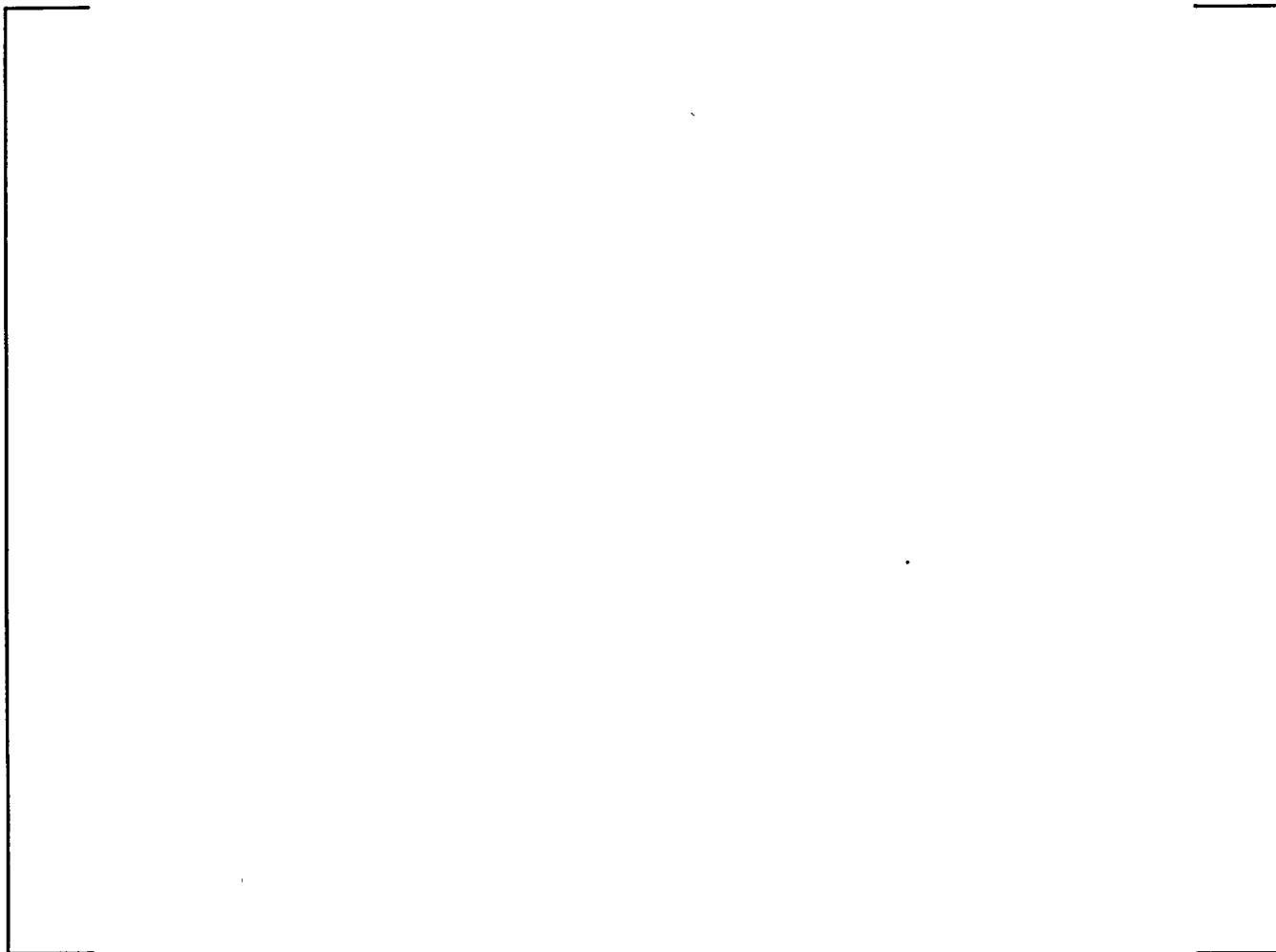


Figure 7.3-10
Static Pont-to-Point In-plane Displacement Vectors
of Rows 58/59 U-bend Region Separated and
Intact Tubes For [

]^{a,c,e}



Figure 7.3-11
Time History Displacement Response of Rows 4/5
Separated and Intact Tubes [

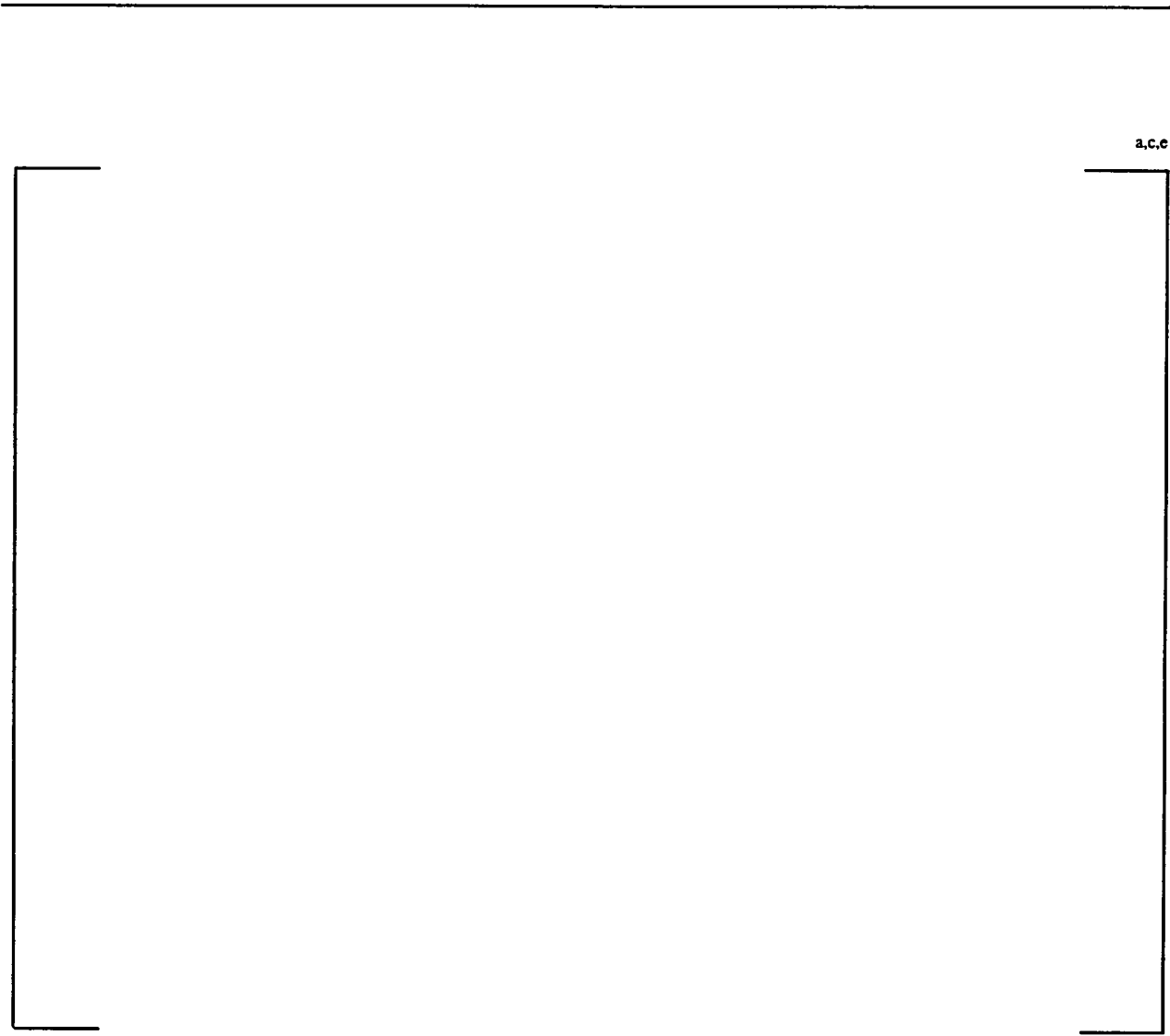
]^{a,c,e}

a,c,e



Figure 7.3-12
Time History Displacement Response of Rows 30/31
Separated and Intact Tubes For [

]^{a,c,e}



a.c.e

Figure 7.3-13
Time History Displacement Response of Rows 58/59
Separated and Intact Tubes for [

] a.c.e

8.0 REFERENCES

- 8.1 NSD-E-SGDA-98-361, 11/98 (Proprietary Report)
- 8.2 WCAP 14797, February 1997 (Proprietary Report)
- 8.3 "Formulas for Stress and Strain", Fifth Edition, Table 32, Cases 1a – 1d, by R. J. Roark and W.C. Young, McGraw-Hill Book Company, New York, NY, 1975
- 8.14 ASME Boiler and Pressure Vessel Code Section III, "Rules for Construction of Nuclear Power Plant Components," 1989 Edition, The American Society of Mechanical Engineers, New York, NY
- 8.5 "Stress Analysis of Thick Perforated Plates", PhD Thesis by T. Slot, Technomic Publishing Co., Westport, CN, 1972
- 8.6 Calculation Note SM-94-58, Rev. 1, A. L. Thurman, Westinghouse, NSD, October, 1994 (Proprietary Report)
- 8.7 Report DE-LAN-765(80), "Determination of Contact Stress Between Tube and Tubesheet of a Hydraulically Expanded Joint", by L. A. Nelson, Westinghouse NTS, January 1980. (Proprietary Report)
- 8.8 General Design Specification 953236, Rev. 1, "Model F Steam Generator Reactor Coolant System", Westinghouse Energy Systems, March 6, 1981 (Proprietary Report)
- 8.9 Systems Standard 1.3F, Rev. 0, "Nuclear Steam Supply System - Reactor Coolant System Design Transients for Standard Plants with Model F Steam Generators", Westinghouse Energy Systems, March, 1978 (Proprietary Report)
- 8.10 PCWG-2631, 4/2/01, "Category IVP-RCS" (Proprietary Report)
- 8.11 ASME Boiler and Pressure Vessel Code Section XI, "Rules for Inservice Inspection of Nuclear Power Plant Components," 1989 Edition, The American Society of Mechanical Engineers, New York, NY
- 8.12 WCAP-12244, Revision 3, "Steam Generator Tube Plug Integrity Summary Report," November 1989 (Proprietary Report)
- 8.13 M. Harris and C. E. Crede, *Shock and Vibration Handbook*, 2nd Edition, McGraw-Hill Book Company, New York, NY, 1976

8.0 REFERENCES (Continued)

8.14 WNET-180, Volume 10, Revision 1, "Model F Steam Generator Stress Report, Tube Analysis," November 1983. (Proprietary Report)

8.15 Calculation Note CN-SGDA-99-66, Revision 0, October 1999. (Proprietary Report)